VOLUME 23, 1961/62, No. 2 pp. 29-68 Published 7th December 1961

Philips Technical Review

DEALING WITH TECHNICAL PROBLEMS
RELATING TO THE PRODUCTS, PROCESSES AND INVESTIGATIONS OF
THE PHILIPS INDUSTRIES

Photo S. T. Karlsson

ELECTRONICS IN THE WOOD INDUSTRY

by M. HAMMAR *), A. RYDAHL *) and B. WESTERLUND *).

621.38:674

Production methods in many industries are changing rapidly with the wide introduction of electronics. Examples include photoelectrical devices, high-frequency heating, telemetering, and control and automation systems. It cannot be the aim of a single article to attempt a survey of the industrial applications of electronics, even for the case of a single industry — the wood industry. Neither does the present article deal extensively with specific electronic equipment, although here and there some details are discussed. The purpose of the article is rather to illustrate the various ways in which industrial processes can be improved by the application of electronics. The nature of the material handled in the wood industry — living matter, with all its freakishness in composition, shape and properties — lends a special flavour to the problems encountered here.

The topics dealt with in this article represent part of the

*) Svenska Aktiebolaget Philips, Stockholm.

activity of Svenska AB Philips, Stockholm in developing "tailor-made" industrial electronic equipment. One reason for focusing attention on Sweden is the important world role of the Swedish wood industry: in 1957 Sweden ranked third of all countries in the production of pulp and fifth in the production of semi-finished and finished coniferous wood products, and in exports of these goods it ranked first and second respectively. Another reason is the fact that wages in this country, being the highest in the world next to U.S.A. and Canada, are fostering investments in equipment for saving labour and increasing productivity. Sweden may therefore be regarded as a "pilot land", foreshadowing the developments in other countries.

Introduction

The three main Swedish industries are mining, steel and wood. In each of these industries, electronic equipment is being used more and more. Conditions in Sweden are favourable for such a development: there is a demand for high output and high quality, which makes new means to these ends welcome, and the introduction of new equipment is stimulated by the pressure of high wages and by the readiness of the manufacturers to pool their knowledge. (Technical collaboration has a long history in Sweden: in the iron industry it began in 1747, and the wood industry has had common research establishments for many years.)

The wood industry is particularly interesting because of the variety of its products, semi-finished or finished — ranging from planks, mining props and telephone poles to pulp, board and paper, and from matches, toys and shoe lasts to parquet blocks, furniture and prefabricated houses. These products constitute about 25% of the total value of Swedish exports. Many of the processes in the wood industry have already been mechanized to a high degree. The help that electronics can nowadays offer in the wood industry is chiefly concerned with two types of operations: *a*) physical ones, including *drying* and *gluing*, for which the required heat can very effectively be produced in a high-frequency furnace; and *b*) organizational ones, including *inspection*, *sorting*, and *control*. The latter group of operation are usually preceded by *measurements* which, again, may involve electronics.

We shall not dwell here on the process of *gluing*, since this important application of high-frequency (dielectric) heating was introduced many years ago and has already been described in this journal [1]). We may however mention that in the past few years installations have been designed in which high-frequency gluing is performed as a *continuous* production process, the objects to be glued being transported through the high-frequency oven on a conveyor belt [2]). A similar procedure, which greatly improves the economy of the process, is adopted in one case of high-frequency *drying*, a comparatively new development which will be described in this article. After this, several examples of electronic *inspection* and *sorting* will be presented. Finally, the complete production process in a *sawmill*, where electronics is put to work at a number of stages, will be considered.

High-frequency drying of shoe lasts

Lasts are the basic tool for the mass manufacture of shoes. When the model for a certain type of shoe in a given size has been designed, a steel prototype of the required last, on which the upper leather will be moulded, is made on a precision milling machine. The requisite number of wooden lasts is then manufactured from this prototype by means of a copying machine. The very strong, hard wood of the beech is generally used for the lasts, since they must remain smooth and retain the designed shape very accurately during the moulding of the leather, the nailing on of the soles, etc. Two or three hundred shoes can be made on a properly manufactured last of this material.

The wood to be machined must have a very low moisture content (7-9%), in order to prevent subsequent shrinking or warping of the last. This would of course affect the correct shape and size, and it would endanger the precise fit of those parts of the last which must be detachable or movable in order to enable it to be withdrawn from the completed shoe.

The rough cut blocks, which may originally contain as much as 65-75% of moisture, must be dried very cautiously, because of the danger of cracking. This danger is enhanced by the very hardness and density of the beech wood which make it so suitable for lasts. Natural drying is a very slow process and cannot reduce the moisture content to less than 30 or 20%. Moreover, when drying proceeds very slowly, there is a risk that the wood will be attacked by fungi ("blue stain" or mould). Artificial drying is therefore the usual practice in many branches of the wood industry. A great number of procedures have been developed for this purpose [3]), the most common

[1]) Philips tech. Rev. **11**, 239, 1949/50.

[2]) See e.g. G. Wästberg, Die Hochfrequenz-Holzverleimung in Schweden, Holz als Roh- und Werkstoff **16**, 177-183, 1958.

[3]) See e.g. F. Kollmann, Technologie des Holzes und der Holzwerkstoffe, Springer, Berlin 1955, Vol. 2, pp. 255-380.

method consisting in heating the wood by a mixture of steam and air in such a way that the outer layers of the wood do not start giving off water before the inner layers have also warmed up and can participate in the process of evaporation (and shrinkage!). Dielectric heating in a high-frequency field is clearly much better suited for the purpose: the heat is not applied from the outside but is developed in the material itself, and the innermost parts of the wood acquire an even higher temperature than the outer layers, which are cooled by the surrounding atmosphere. The water from the middle is thus the first to evaporate and it can find its way out relatively unimpeded through the pores of the outer layers, which have not yet shrunk.

The high-frequency drying of wood, first conceived in 1928 in the U.S.A. and extensively investigated since 1934 in Russia, Germany and other countries [3]), is relatively expensive, but so are the losses that may be inflicted by other drying procedures. Moreover, high-frequency drying is much faster than other methods. It will therefore be an economic proposition in many cases, and especially for small, carefully machined objects such as shoe lasts. Moreover, recent developments have considerably improved the economy of high-frequency drying by making the process *continuous*: the material is then transported on a conveyor belt through the high-frequency field of an open capacitor. Svenska Skolästfabriken at Järrestad in the south of Sweden have used such a method for the last two years with considerable success. A few details of their installation [4]) (*fig. 1*) are given here.

The high-frequency generator operates at 12 Mc/s and delivers 20 kW of HF power. It comprises a power-supply unit with a high-tension transformer and a 3-phase full-wave rectifier, and a HF unit with an oscillator tube and an oscillating circuit in which the oven serves as the capacitor (*fig. 2*). The oven contains one lower electrode about 3 metres long (perforated so that the water can drain off), over which the conveyor belt (of fine-meshed stainless-steel gauze) carrying the wooden blocks is passed, and three upper electrodes each about 1 metre long. The three upper electrodes are interconnected by flexible sheets and are separately adjustable in height. This subdivision of the capacitor into three independent sections is necessary in order to control the HF field strength and thus the degree of heating the blocks will undergo at different

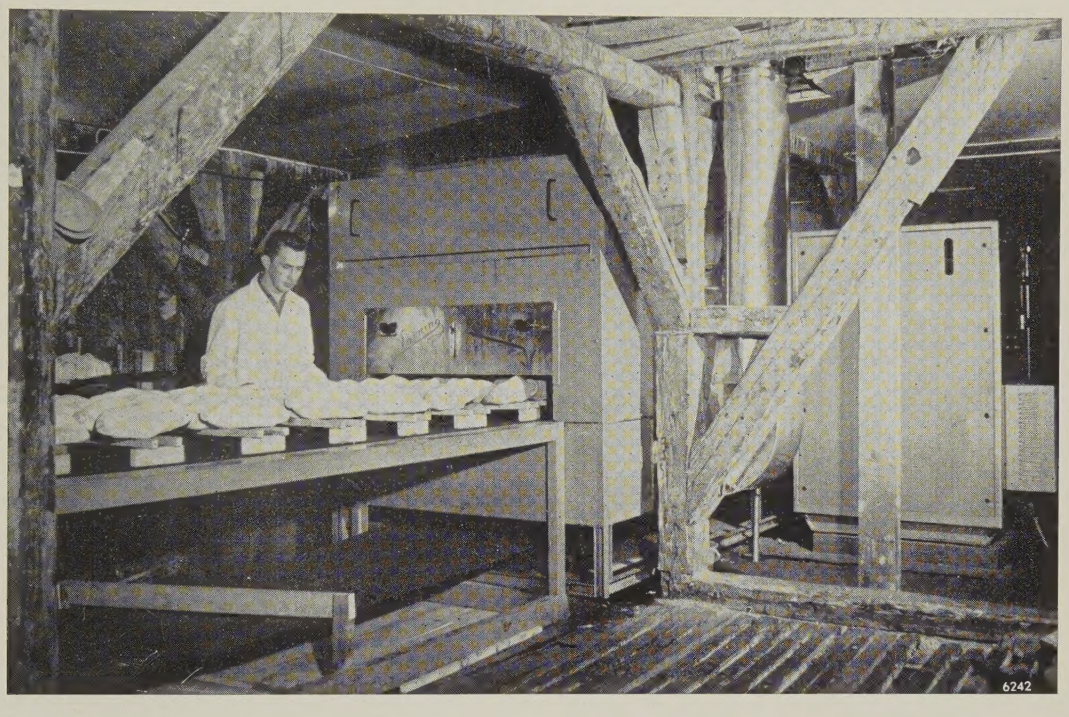

Fig. 1. Installation for high-frequency drying of shoe lasts at Järrestad, designed by Svenska AB Philips, Stockholm in collaboration with Svenska Skolästfabriken. The belt loaded with lasts travels through the HF oven at about 3 m/hour. To the right, the 20-kW HF generator.

[4]) Designed in the HF-heating laboratory of Svenska AB Philips, Stockholm in conjunction with Svenska Skolästfabriken. A series of identical installations are being built for other plants in collaboration with this company.

points when travelling through the oven; they should be heated strongly in the first section of the oven, then given a "rest period" with moderate heating, while in the last section the heating should

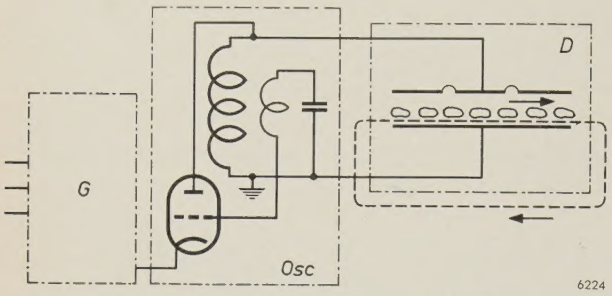

Fig. 2. Circuit diagram of HF generator and oven. *G* power-supply unit. *Osc* HF unit. The large capacitor which forms part of the oscillating circuit is situated in the oven *D*.

increase again. The design of the HF circuit had to allow for an unusually large spacing between the upper and lower electrodes of the capacitor (*fig. 3*): the water dripping from both ends of the wooden blocks must be prevented from short-circuiting these with the lower electrode, as this might cause the wood to be overheated in places, or even to burst into flame. The upper electrode must also be a considerable distance above the blocks in order to avoid excessive fields on protruding ribs and points.

Since between 500 and 800 grams of water normally have to be removed from each block, while the 20-kW oven can remove a total of 35 kg of water per hour, an average of 30 pairs of lasts can be dried per hour. About 10 pairs can usually be accommodated per meter of the conveyor belt, so that the belt can move at a rate of about 3 m per hour. During the passage through the oven each block shrinks by about 12% in width and 6% in height (*fig. 4*). Thermo-couple measurements have shown that the HF field heats the middle of the block to 85 °C, and its surface to 50 °C.

The complete drying process established at Järrestad after a certain period of experimentation is represented in *fig. 5a*. The blocks of wood are taken from stock after 2 months of cold storage, when the initial moisture content of 62% has dropped to 35-50%. They are then stored at room temperature for about 2 days (pre-drying), HF-dried in less than 2 hours, and again stored at room temperature for 1 or 2 days before machining, in order to allow the wood to cool down and to allow the remaining moisture content of about 7-9% to distribute itself uniformly. This procedure should be contrasted with that in use before the introduction of HF drying (see fig. 5*b*): the blocks had to be kept in cold storage for 6 months, were then dried by hot air for 3 months, and finally stored at room temperature for 1 month.

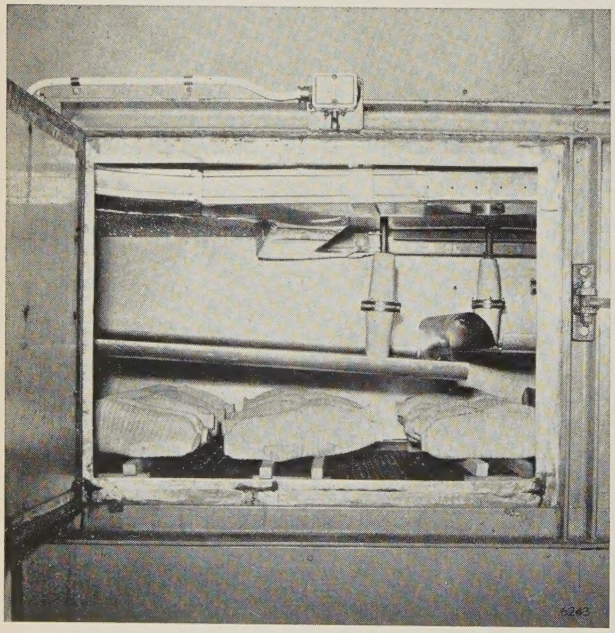

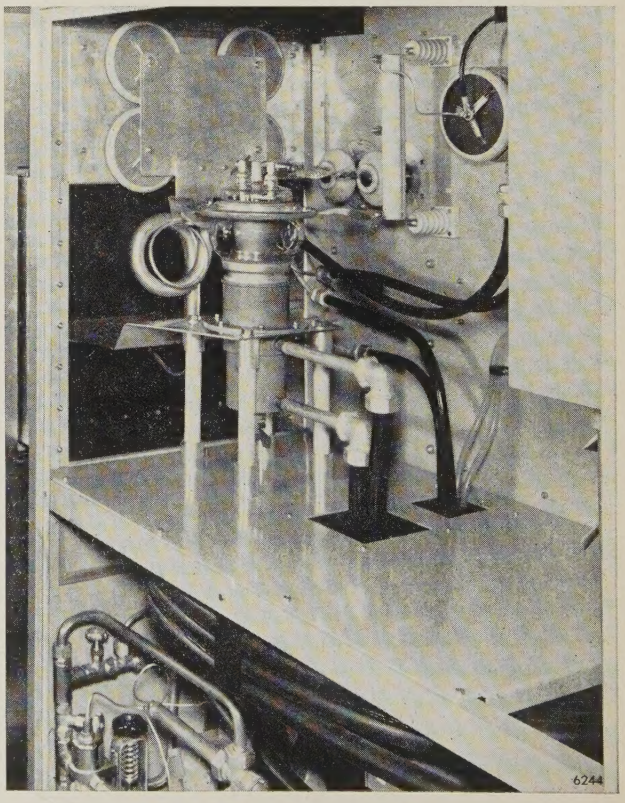

Fig. 3. Installation for the high-frequency drying of shoe lasts: interior view of the HF cabinet of the generator (right) and the oven with electrodes (above).

A comparison between the times involved bespeaks the advantage of HF drying quite eloquently: the wood stocks and storage space required for a given output are enormously reduced. Storage costs at Järrestad have been brought down to 15% of their former levels. (The saving of the energy formerly used for heating the hot-air drying chambers is not a real advantage, since this energy

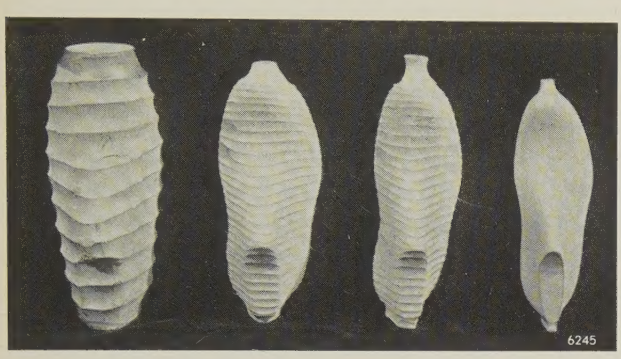

Fig. 4. Four lasts in different stages of manufacturing. From left to right: rough cut block; a similar block roughly machined to the shape of the last, before drying; the same after drying; machined to final shape.

was provided extremely cheaply by burning scrap wood.)

This large saving is obtained at a relatively low investment cost, thanks to a change in the manufacturing process made possible by the new drying method. The blocks of wood cut from the trees must be large enough to accommodate every type and size of last. With the former method, where the drying period was much longer than delivery times scheduled for batches of lasts, it was unavoidable that a large quantity of wood in each block was kept in the drying process, taking up space in the store and in the hot-air chambers, only to be removed in the preliminary and final machining of the block. With HF drying, blocks selected for a batch of lasts (after 2 months' storage) can be roughly machined *before* passing through the HF oven (see fig. 4), thus considerably reducing the quantity of wood to be dried and therefore the size and power of the HF generator to be installed for a given production.

Other advantages arise in addition to the savings in storage costs. The long drying periods previously used could not prevent the rejection rate because of cracks from amounting to 8-10%; the rejection rate because of fungi was sometimes even higher. With HF drying, only 1-2% of the blocks have to be rejected for cracks, and none for fungi. Moreover, the HF-dried wood is found to be definitely of superior quality: it is brighter, more uniform in colour and in strength, and easier to machine and to polish. The latter advantages could hardly have been predicted, although wood experts state that they can be explained by considering the microprocesses occurring in the wood during drying. This, however, is taking us beyond the scope of this article.

Inspection of veneer for match boxes

The manufacturing of matches was one of the first industrial processes to be virtually completely mechanized. A large number of single steps are involved and a variety of machines are used for performing them. The logs (aspen wood is generally used) are peeled to produce veneer of two thicknesses, one for the match sticks, the other for the

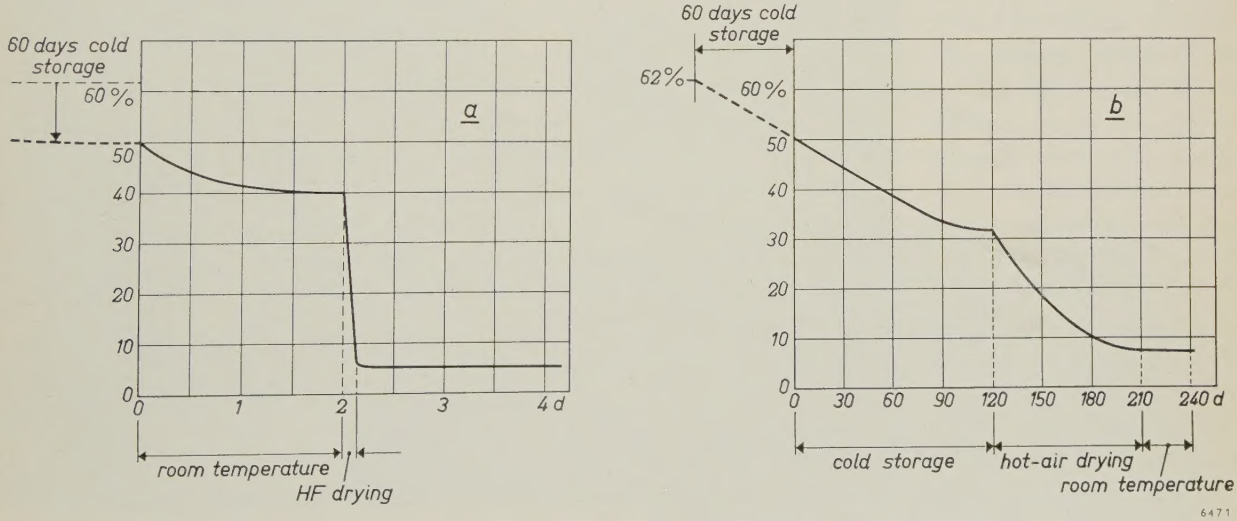

Fig. 5. *a*) Time diagram of new drying process for lasts at Järrestad: water content of the wood in wt.% as a function of time in days, beginning after two months' cold storage. *b*) Time diagram of old drying process. Cold storage actually lasted for 6 months, but the first two months are put before the zero of the time scale, to make the two graphs comparable.

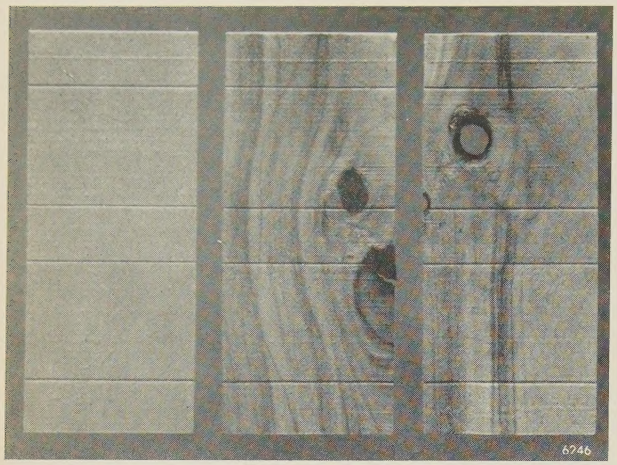

Fig. 6. Strips of veneer for the sleeves of match boxes. Each strip is folded along the grooves. From left to right: normal strip; strip with knot; strip with hole.

match boxes. After the veneer has been cut to the required lengths, it follows two separate lines. The first line includes: cutting the veneer strips to obtain the match sticks (one machine will make as many as 70 million a day); collecting, drying and chemically polishing and impregnating the sticks; eliminating short and faulty ones; aligning the sticks parallel and passing them through an enormous dipping machine for providing them with the heads, hardening these in an adjacent drying installation and collecting the finished sticks for filling the boxes. The second line makes the boxes: the veneer strips, coming in two widths, narrow for the drawer, broad for the sleeve, both already grooved during cutting, are fed to two separate machines. These will fold them (at a rate of 200 per minute), add the cardboard bottom for the drawer and paste paper strips on to them, whereafter the sleeve is completed by pasting on the colourful emblem and painting the striking surfaces on both sides. Box and sleeve are finally fed to the filling machine to meet the sticks.

Very little manual labour is involved in this manufacturing process: 3 man-seconds are required for one match box, completed, filled with its 50 sticks and packed.

About 10% of this labour is spent on one seemingly very simple step: inspecting the veneer for the boxes and removing those strips containing knots, holes or other visible defects (*fig. 6*). The girls in charge of the folding and pasting machines let the piled-up strips of veneer pass through their fingers like a fan and drop every defective one with a quick movement. One girl can look after and feed two machines, about half her time being occupied by inspecting and sorting the veneer strips, at a rate of 400 per minute.

However elegantly the girls perform their task, it is evident that here is a point where electronics comes into its own: the inspection can be done photoelectrically and the removal of the defective strips can be effected with the aid of a relay. Equipment which performs this task for the broad veneer

Fig. 7. Folding machine for match-box sleeves at the Vetlanda factory of Svenska Tändsticks AB. Top centre, the magazine for the strips of veneer (the girl is holding another stack of strips to fill the magazine) and the box containing the scanning mechanism for inspecting the strips. To the right a defective strip is just leaving the slide and entering the chute to the reject box.

strips has been designed and installed for Vetlanda Tändstickfabriken, a member of the group Svenska Tändsticks AB, Jönköping. A considerable number of instruments of the same type will in due course be installed in the factories of this group in consequence of the very satisfactory results obtained with the prototype. The apparatus is shown in action in *fig. 7* and will now be described briefly.

The strips of veneer contained in the magazine of a folding machine are passed in rapid succession over a smooth metal surface (the "slide") by several pairs of rollers. A photoelectric cell above the slide observes the light reflected from the moving strip when this is scanned in the transverse direction by a flying spot. (In reality, there are two scanning spots, see below.) If the strip of veneer is faultless, the photoelectric current will be approximately constant and the strip passes on to the folding mechanism. If, however, the scanning spot passes a knot, which is darker than the normal wood (or a hole, whose edges likewise are darker), the photoelectric current diminishes suddenly, and by this negative pulse actuates a relay, energizing a solenoid which raises a hinged steel plate at the end of the slide, causing the defective strip of veneer to enter a chute leading to a reject box. 700 scans, covering six pieces of veneer, can be carried out per second.

An interesting point in this rather commonplace set-up is the solution of the well-known problem of the spurious pulse produced at the edges of the scanned object: every time the flying spot crosses one of the edges, it gives rise to a signal similar to that indicating a knot or hole, so that every strip would be discarded unless special precautions were taken. Keeping the spot exactly within the width of the strips is hardly possible. The difficulty is eliminated in a simple way by using *two* alternating scanning spots, which move in opposite directions. The photocell current caused by each spot is initially suppressed until the spot is well on the strip, but is allowed to flow until the spot has pursued its course well beyond the far edge. The slide on which the strips move has a *brighter* surface than the veneer. Every time a spot leaves the strip a *positive* current pulse is now delivered by the photoelectric cell, but this is made ineffective by a simple circuit, which causes the above-mentioned relay to react only to negative pulses.

The two flying spots are produced by means of a small light bulb surrounded by a rotating perforated drum and flanked by two stationary mirrors; the arrangement is shown in *fig. 8* and a few details are explained in the caption. *Fig. 9* shows the device in its cover and the cabinet containing the electronic circuits.

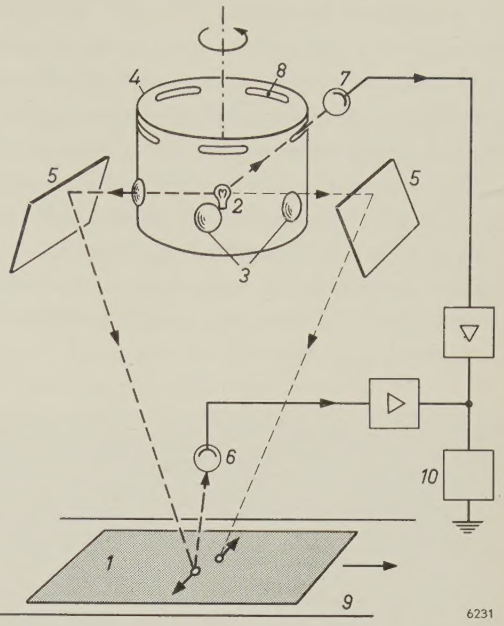

Fig. 8. Scanning system for the inspection of veneer strips. Two flying spots appearing alternately on the strip *1* and moving in opposite directions are produced by the lamp *2* by means of lenses *3* in the rotating drum *4* and fixed mirrors *5*. The photocell *6* receives the reflected light of the spot and produces a negative current pulse firing a thyratron and thereby actuating the reject mechanism as soon as a dark part is encountered in the strip. Until each spot has crossed the first edge of the strip, the photocell current is suppressed by the signal of the auxiliary cell *7* illuminated by suitably phased slits *8* in the rotating drum. The positive current pulse produced by *6* at the moment when each spot crosses the second edge of the strip and arrives on the brighter surface *9* underneath is made ineffective by a diode in the thyratron circuit *10*.

Owing to the introduction of this automatic inspection equipment, one girl can now run 4 machines instead of 2. For the time being, only the *broad* veneer strips used for the sleeves of match boxes are sorted in this way. Similar equipment for inspection of the narrow strips for the drawers is being developed.

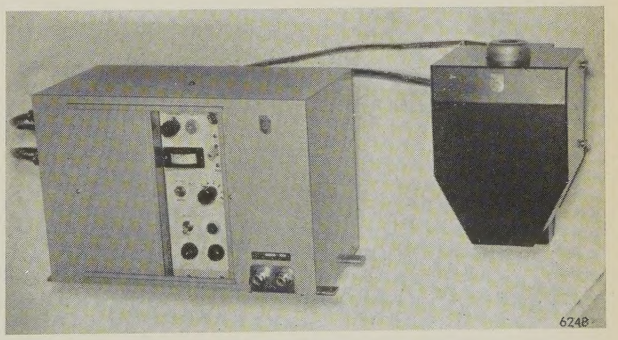

Fig. 9. Scanning device in its cover (right) and cabinet with electronic circuits.

Sorting of parquet blocks

The following example is not very different in principle from the one just discussed, but it illustrates the possibility of more sophisticated scanning, adapted to the variety encountered in the appearance of wood. This example concerns equipment developed and installed for Limhamns Träindustri at Ronneby, where it has been working for more than a year. The equipment automatically sorts oak parquet blocks into four different classes, viz., bright, medium, dark, and patterned (*fig. 10*).

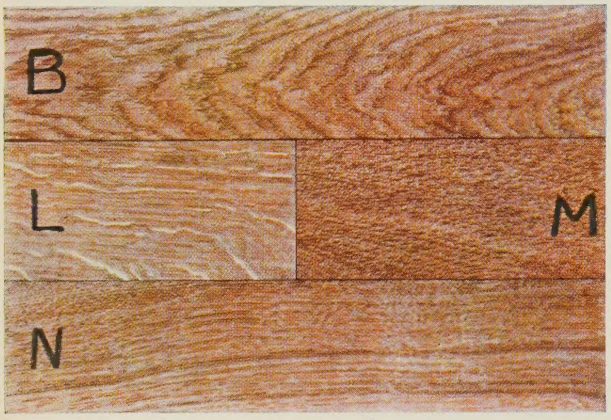

Fig. 10. Oak parquet blocks of four different classes: *L* bright, *N* medium, *M* dark, *B* patterned.

Blocks of fixed dimensions (length between 20 and 45 cm, width between 5 and 8 cm) are fed into a magazine, from which a conveyor belt takes them, one after another, to a photoelectric scanner. The scanner contains two photocells (*fig. 11*). The first cell measures the average brightness (reflectivity) of the block as it passes under a uniformly illuminated window of length 10 cm and width equal to that of the block. The reflectivity limits for the medium class can be preset within a wide range. The blocks which are darker or brighter than these limits are assigned to the dark class and the bright class respectively. This information, conveyed by the photocell current, is stored for a short time in an *RC*-type "memory": it will actuate a mechanism depositing the block in one of three boxes which it will pass when it is carried further by the continuously moving belt. Before this happens, however, the block passes under the second photocell, where it is scanned by a light spot with an area of 3×5 mm, reflected from a rotating mirror and thereby describing a circular path on the block. If the wood has a pattern of darker and brighter lines, the photocell observing the light reflected from the block will deliver an alternating current, whose amplitude will be larger the more pronounced the pattern. By amplifying this current and passing it through a suitable circuit (similar to the clamping circuit well known from television techniques), a current of the shape shown in *fig. 12* is obtained and fed into an integrating *RC* circuit. If the voltage on the capacitor reaches a certain (adjustable) value, the information concerning the average brightness, previously stored in the memory, is cancelled and replaced by a signal which will deposit the block in a fourth box, for the "patterned" class.

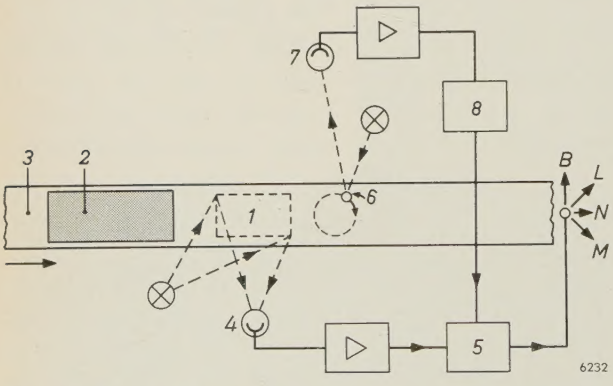

Fig. 11. Scanning system for sorting parquet blocks. *1* uniformly lit window, underneath which the blocks *2* are transported by belt *3* and which is observed by photocell *4* for measuring the average reflectivity of each block. The signal produced is stored in the memory *5*. The scanning spot *6* produces a varying signal in photocell *7*, which is integrated in *8*. If the integrated signal exceeds a certain limit it replaces the signal stored in *5*. The output of *5* controls the position of "points" directing the blocks to boxes *L*, *N*, *M* or *B*.

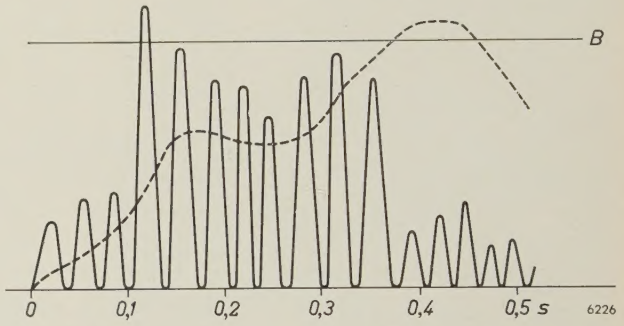

Fig. 12. Signal obtained when the scanning spot moves on a block. The broken line is the integrated signal, which must exceed the limit *B* for the block to be classified as "patterned".

The apparatus is illustrated in *fig. 13*. The sorting speed is about 1 block per second.

The obvious advantage offered by electronic sorting is again the saving of labour, but it should be emphasized that the improvement of quality is of equal or even greater importance: substituting physical criteria for the subjective comparison in the evaluation of brightness and variegation contributes greatly towards obtaining a more uniform product.

Electronic equipment in a sawmill

In order to illustrate some of the roles electronics can play in a sawmill, the complete production

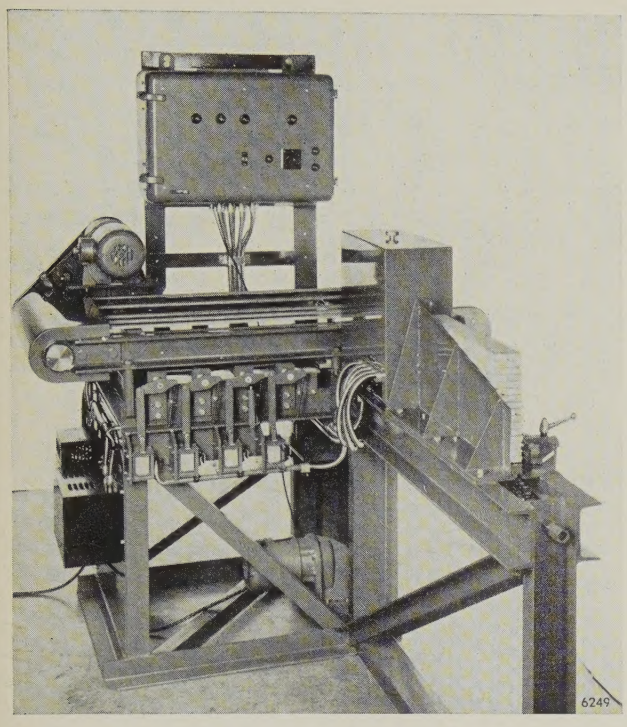

Fig. 13. Equipment for sorting parquet blocks installed for Limhamns Träindustri at Ronneby.

process in such a plant will be described, with special reference to the sawmill of Domsjö Såg at Örnsköldsvik in the northern part of Sweden, which is part of the group Mo och Domsjö AB. This mill, one of the largest of Sweden, with an annual output of 17 000 standards [5]), has been using two large electronic installations for sorting logs and boards for the past few years.

The logs arriving at the plant from the forests have to undergo three main operations: debarking, sawing and drying. The initial stages of this sequence at Domsjö Såg (and also at other large sawmills) are largely based on the availability of a large harbour basin, since the logs are more easily manoeuvred in water than on land. A large part of the logs to be sawn actually arrive at the mill in enormous floats (title photograph). The logs arriving by truck — about half of the total number at Domsjö Såg — are also usually unloaded into the harbour basin. Freezing of the harbour basin during the winter is therefore a serious though unavoidable drawback of the geographical situation of most Swedish sawmills. In order to postpone freezing for as long as possible, the water is stirred in some cases.

Let us now follow the logs on their way through the plant (see the "flow diagram", *fig. 14*). When the logs have been taken from the truck or the float, they will be put on a conveyor belt carrying them to the debarking machine. Before this is done, half of them must be turned round: they must enter the debarking machine narrow end first, but during transport half of the logs point one way and half the

[5]) 1 standard is equal to 4.672 m³ and corresponds to 40-50 logs.

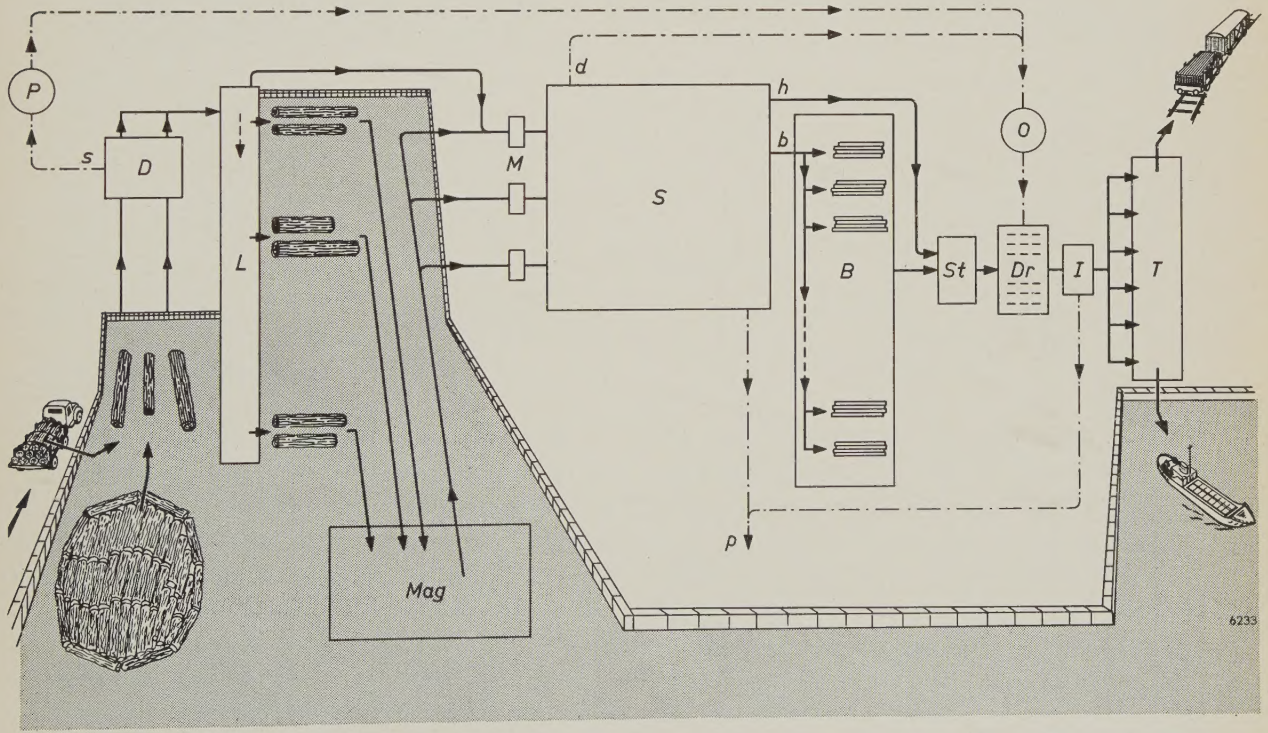

Fig. 14. Flow diagram of the sawmill of Mo och Domsjö AB at Örnsköldsvik. *D* debarking machines. *L* log-sorting installation. *Mag* magazine for sorted logs. *M* metal detectors. *S* sawing lines. *B* board-sorting installation. *St* stacks of boards. *Dr* drying plant. *I* final inspection. *T* storehouse for boards. *P* press for bark *s*. *O* boilers using dry bark and sawdust *d* as fuel. *h* heart planks, *b* boards, *p* scrap wood for pulp. The process in the block marked *S* is explained in the text with reference to fig. 16.

other. The bark removed during debarking is compressed and used for fuel. The logs coming from the debarking units (two at Domsjö Såg) are put on a common platform where their diameter at the narrow end is measured. This measurement places each log in one of 23 thickness classes, corresponding to 23 bays arranged on a line 200 m long in the harbour basin. The logs are then put on a conveyor running along these bays and are automatically unloaded into the right bay by means of electronic sorting equipment. This equipment will be described below in some detail. About 3400 logs are sorted in an 8-hour shift in this way at Domsjö Såg. When a bay has been filled with logs, they are tied together with chains and taken away by a tug-boat for storage in a magazine occupying part of the harbour basin until their class is selected for sawing.

The logs to be sawn are towed or floated to the conveyor belt for the frame saws. Domsjö Såg is equipped with three complete sawing lines, each fed by a separate conveyor. Before entering the sawing line each log is passed through an *electronic metal detector* for indicating logs containing large nails or other metallic objects which might damage the saw blades (*fig. 15*). (In some sawmills, the metal detector is situated before the debarking machine.)

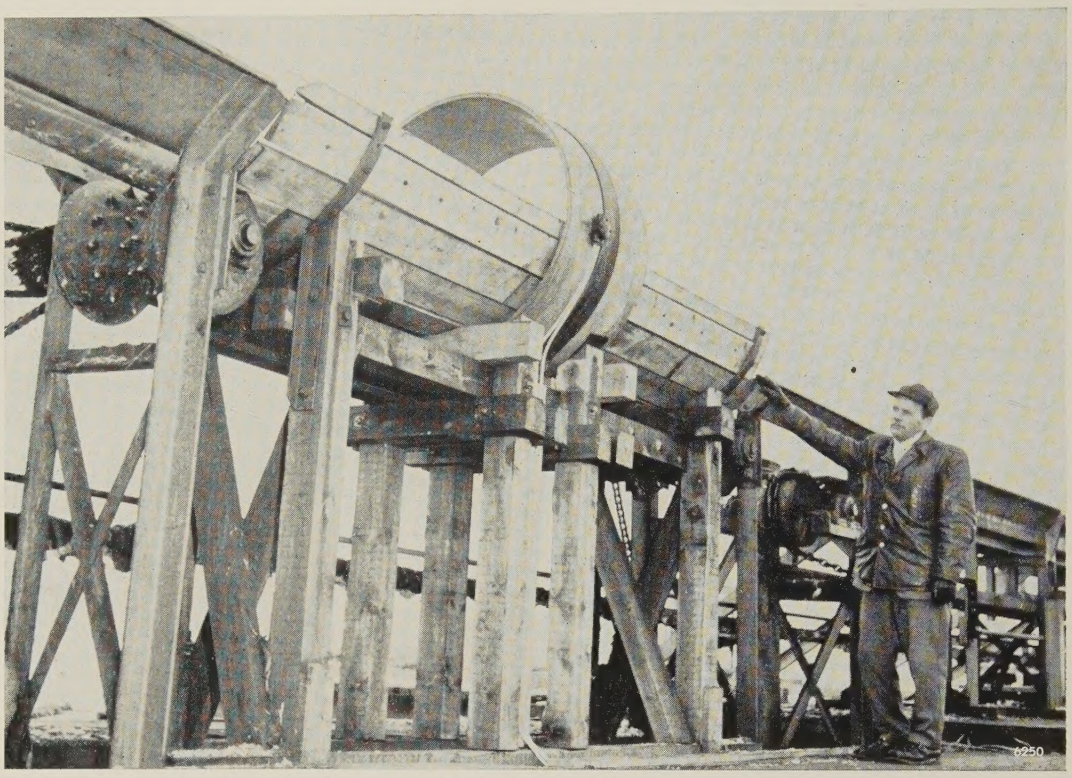

Fig. 15. Metal detector, in use in the sawmill of Tunabergs Trävaru AB at Koppartorp. The logs on their way to the saws are transported on a non-metallic conveyor through the coil 1 metre in diameter seen in the centre of the picture. Logs containing big nails or other metal objects that might damage the saws change the inductance of the coil during their passage and thereby actuate a relay giving an alarm signal. (The relay in some installations causes a paint gun to produce a spot on the log at the location of the metal, or it causes the log to be put off the conveyor.)

Although the principle is well known and has been applied in many other fields (see e.g. E. Blasberg and A. de Groot, Metal detectors, Philips tech. Rev. **15**, 97-104, 1953/54), the design and the installation for the present application is relatively difficult: because of the large coil diameter required and the small dimensions of the objects to be detected, the apparatus must be made very stable electrically and mechanically. The latter requirement is quite a problem in a sawmill.

After sawing, the planks or "boards" are sorted according to their thickness and width. This is done in another large sorting plant, using an electronic control system, which will also be described below. Next, the boards are loaded on to special trucks carrying 3 standards each and transported to the drying plant. The importance of artificial drying in fighting blue stain and mould has already been stressed in the first section of this article. The drying plant of Domsjö Såg operates on hot air and contains 8 channels, each taking 15 stacks of boards. The plant has a capacity of 70 standards per 24 hours.

After cooling down, the dried boards are transported to a platform, where a final inspection takes place, poor ends are cut off and the boards are marked according to quality and size. They are then taken to the storehouse on the waterfront, from where they will be shipped in due time.

We shall presently describe the log-sorting plant. Before doing so, however, we must explain what purpose is served by such a gigantic sorting operation. To understand this, we must first consider the sawing strategy. This strategy most visibly influences the course — and the economics — of the whole production process.

The usual method for most large sawmills is "block sawing"; see *fig. 16*. A log, of length varying between say 9 and 21 feet, is put on a carriage and is passed through a reciprocating frame saw containing a number of parallel saw blades, which simultaneously cut a number of boards from two opposite sides of the log. These boards originating from the rounded parts must be severely cut down in subsequent "edging" machines, and they will usually finish up shorter than the log because of the taper of the tree. The remaining main part of the log is turned through 90° and passed through another frame saw. Again, only thin and relatively short and narrow boards can be obtained from the rounded sides cut off by the outermost saw blades. The spacings of the saw blades in both frame saws should be chosen such that the heavy "heart" planks (fig. 16*a*), which do not need subsequent edging and represent the most valuable part of the log, will be as wide and thick as possible, while at the same time the sides of the log should also be used to the greatest advantage, with the least possible amount of scrap wood. The best compromise for a given taper and average "crookedness" of the relevant type of tree is a matter of experience — although ideas of putting electronics to work for this task too are being considered.

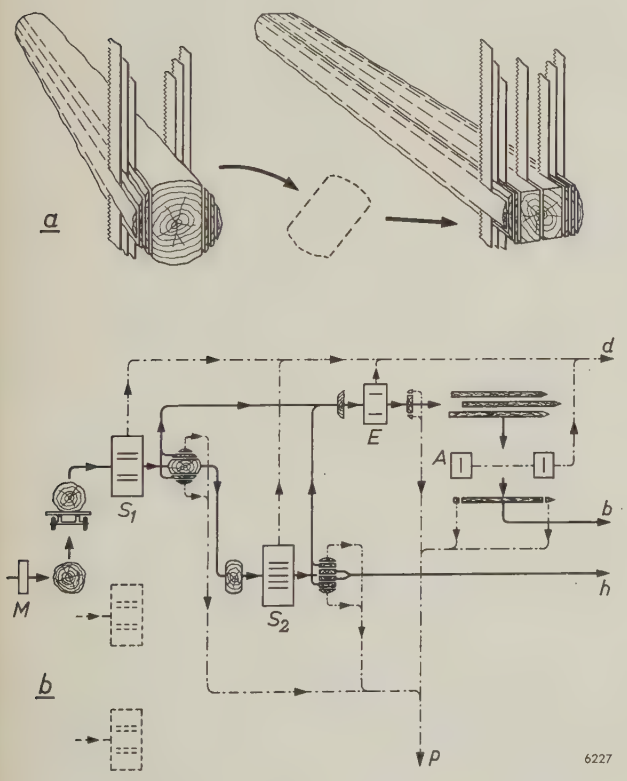

Fig. 16. *a*) Block sawing. A log is first passed through a frame saw which simultaneously cuts a number of thin boards from both sides (left); then it is turned through 90° and passed through a second frame saw (right). The thinner boards must be "edged" and "adjusted". The whole process is diagrammatically represented in figure (*b*), which represents the contents of block *S* in the flow diagram of fig. 14. *M* metal detector. S_1 and S_2 frame saws. *E* "edging" saws. *A* "adjusting" saws. *h* heart planks, *b* boards, *p* scrap wood for pulp, *d* sawdust.

It follows from the above that the spacings of the saw blades in each frame saw must be carefully adjusted in accordance with the *thickness of the log*. The sawmill must of course deal with logs of widely varying diameter, ranging e.g. from 5 inches to 18 inches. In order to avoid frequent changing of the adjustment of the saw blades, the logs are sorted into a number of thickness classes and one sawing line is fed logs of one thickness class for at least one shift, in some cases even for several days on end.

The sorting of the logs

A sketch of the lay-out of the log-sorting installation is given in *fig. 17*. *L* is the sorting platform where the logs are measured. The operator is seated at a desk carrying 23 buttons which correspond to the 23 thickness classes [6]) into which the logs must be sorted (*fig. 18*). In an adjacent cabinet a paper strip about 10 cm wide, on which 23 parallel "tracks" are available, moves beneath a row of 23 punches at a very low speed, about 2.5 mm/sec (*fig. 19*). The movement of the paper strip is geared directly to that of the conveyor belt running along the platform (the speed of the conveyor belt is about 1.2 m/sec). As soon as the thickness class of a log has been determined — let it be class number *k* —, the log is pushed off the platform on to the moving conveyor, and the operator presses the button *k*. This causes a hole to be punched in the paper strip by punch number *k*. A photocell is placed above each of the 23 tracks of the paper at such a distance from

[6]) A few of these are in reality special categories, such as "crooked" or the like, for logs which have to be diverted from the normal course of sawing.

the corresponding punch that the punched hole will reach the cell and let light fall on to it at the exact moment that the log on the conveyor will have reached the corresponding bay (k). For the most distant bay this will only happen as much as 3 minutes after the log was put on to the conveyor. The current of photocell k then energizes a relay causing a pneumatically or electrically driven lever at bay k to push the log off the conveyor belt into the bay.

The paper strip obviously acts as a delay system for bridging the varying time intervals which pass before each log arrives at the right bay. This mechanical delay system, unusual though it may seem in electronic equipment, is very simple and offers the important advantage that it does not involve any real time relationships but only place relationships: if the conveyor belt is stopped for some reason, the logs resting on it will still be delivered to the right bays when it starts up again.

An interesting detail of the equipment is the fixing of the exact moment when the hole for a log

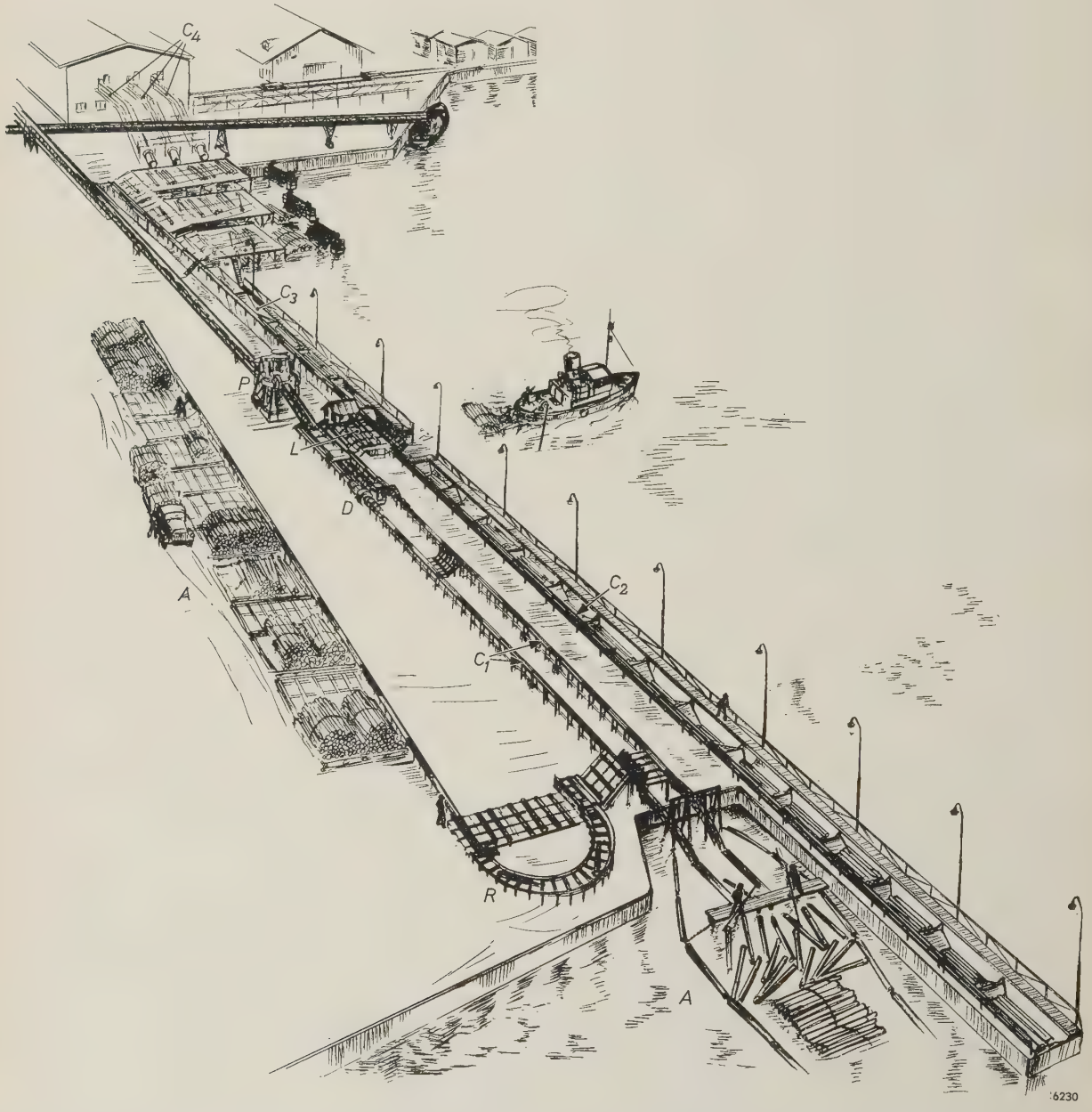

Fig. 17. Log-sorting area of Domsjö Såg. A arrival of the logs by truck (especially in wintertime when the harbour is frozen) or by float. R reversal of half of the logs (shown here as being done on land; more usually done in the water). C_1 conveyors to the debarking machines D. P machine for compressing the bark. L platform where the logs are measured. C_2 conveyor running along the bays for the different classes of logs. (Some of the bays are situated on the other side of L. The logs for these bays are placed on the conveyor C_3, which also carries logs directly to the sawing lines; this trivial complication has been neglected in the further description.) C_3 conveyor running to the sawing plant. C_4 three separate conveyors, each feeding logs to one of the sawing lines. — The conveyors at Domsjö Såg were made by Bahco Erenco AB.

Fig. 18. Operator at desk containing the 23 buttons for directing the logs to their respective bays. The logs arrive from the right-hand side on the platform visible through the window. To the left the conveyor with the 23 bays.

has to be punched into the paper. This moment must obviously be governed not by the operator's action in pressing the button but by the actual arrival of the log at a certain point of the conveyor, say point *C* in *fig. 20*. Moreover, the *length* of the log, which may vary from 9 feet to a maximum of 21 feet, must be taken into account. The bars which push the logs into the water must not be more than about 9 feet long, as otherwise there would be a risk of one bar pushing two logs at the same time. If, on the other hand, a bar of length 9 feet should push a 21-foot log at a one end, this log would fall into the bay at an angle, thus seriously hampering the tying together of the logs in neat bundles. The electronic sorting equipment therefore contains a device which ensures that the hole for each log is punched into the paper at the moment when the mid-point of the log passes the fixed point *C*, so that the pre-determined lever will be actuated at the moment when the mid-point of the log will pass it.

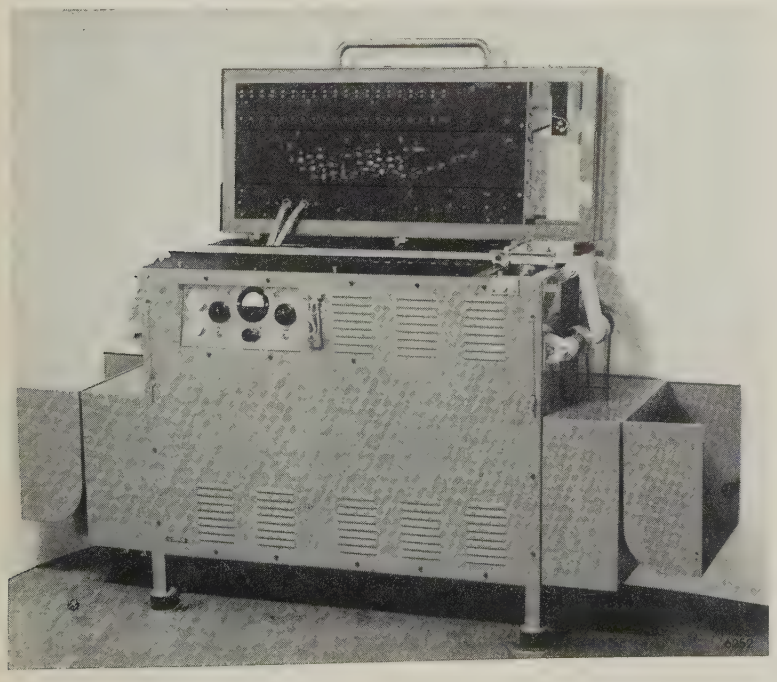

Fig. 19. Cabinet with electronic circuits and the moving paper strip acting as a delay system. A series of punches and the corresponding photocells may be seen arranged on oblique lines in the middle of the lid, which is opened to show the interior. The seemingly haphazard arrangement is in fact chosen with regard to the available space; only the distance between each punch and the photocell on the same "track" matters. (Even with a judicious arrangement, 23 punches cannot be accommodated by one strip. The actual installation for 23 bays therefore comprises two complete delay cabinets. This trivial complication has been disregarded in our description.)

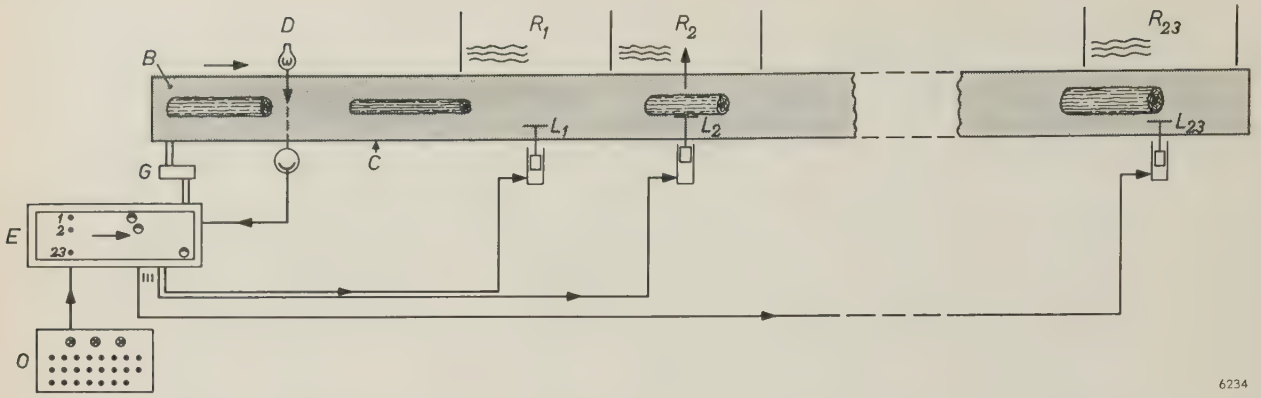

Fig. 20. Log-sorting installation. *O* operator's desk with 23 buttons. *E* cabinet with electronic circuits and paper strip. *G* gearing by which the movement of the strip is coupled to that of the conveyor belt *B*. R_1-R_2-. . . .-R_{23} bays, with pneumatically driven levers L_1-L_2-. . . .-L_{23} for dropping the logs. *D* lamp and photocell of mid-point-seeking device.

This device will be described with reference to *fig. 21*. A beam of light falling on to a photocell is directed across the path of the logs at point *D*, situated a distance equal to half the maximum length of a log (i.e. $\frac{1}{2} \times 21' = 10\frac{1}{2}'$) before *C*. The beam and hence the photocell current will be interrupted by a passing log, and will reappear when the tail of the log arrives at *D*. At this moment the head of a log of the maximum length l_{max} (21′) would be at *E* and its mid-point at *C*, but the head of a shorter log would only have got to *E′*, say, and its mid-point to *C′*. The reappearance of the current cannot thus be used for controlling the actual punching after the operator has pressed the button. Instead, a switching disk is incorporated in the delay-system cabinet, which is started rotating at an angular velocity ω by the disappearance of the photocell current (arrival of the head of the log at *D*) and which switches on the punch after rotating through a certain angle Θ. At the speed ω, the rotation through Θ would be completed when a 21-foot log had the (correct) position *DE*, but the shorter log considered above would then have travelled too far and reached the position *D″E*. The speed of the disk is however *doubled* by the *re*appearance of the photocell current (tail of shorter log at *D*, head at *E′*). The remaining part of the rotation through Θ is therefore completed in a shorter time, namely such that the shorter log will have arrived at the position *D‴E‴*, exactly half-way between the positions *DE′* and *D″E*, and its mid-point will now be at *C*, where it should be at the moment of punching.

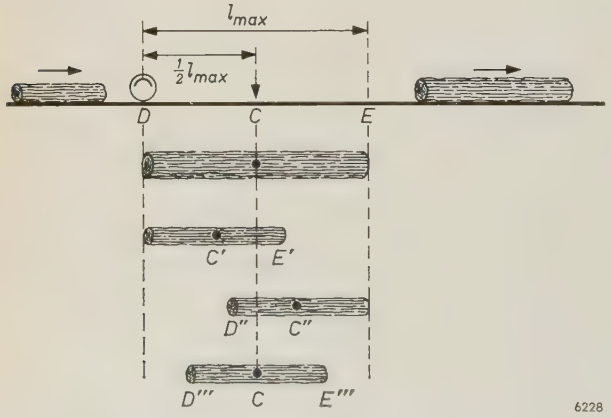

Fig. 21. Diagram for explaining the mid-point-seeking device.

When two relatively short logs are put on to the conveyor in quick succession, it may happen that the head of the second log will arrive at *D* before the switching disk has completed its full rotation for the first log. Another switching disk is therefore provided, the two disks being used alternately by means of an interlocking circuit.

A few more details of the log-sorting installation may be mentioned briefly. The operator has a special button at his disposal for cancelling his last decision, so that — within a certain lapse of time — he can correct an error. Pilot lights indicate the state of affairs. Another special button takes care of the logs in the thickness class being sawn on that day: this button actuates a set of "points", throwing the log on to a subsidiary conveyor belt as soon as it comes off the platform. It is then carried not to the sorting bays but in the opposite direction, to the sawing lines (fig. 17). All the logs sent in either direction are automatically counted. The paper strip of the delay system is stored on a 250-m spool, sufficient for approximately three 8-hour shifts. A sensing lever pressing against the paper on this spool will sound an alarm when a length of paper sufficient for only 15 minutes is left.

The measuring of the diameter of the logs used to be done by means of calipers, or simply by visual estimation after the operator had gained some experience, but an *electronic gauge* has recently been developed for the purpose and installed at one sawmill (*fig. 22*). This instrument quite considerably improves the speed and reliability of the measurement.

Let us now turn to the sorting plant for the boards.

The sorting of the boards

We have already mentioned (page 39) that in block sawing, the spacings of the saw blades in

each frame saw must be carefully adjusted in accordance with the thickness class of the logs being sawn, to make the best use of the wood (cf. fig. 16a). A given setting of the frame saw will give boards of one, two or three different thicknesses in addition to the heavy heart planks. Moreover, the boards of a given thickness will differ in width, depending on how near the edge of the log they were cut, and on the varying degree of edging necessary to remove the curved sides. For one setting of the saw as many as 24 different types of board — different combinations of thickness and width — may be obtained (disregarding the heart planks) [7]).

[7]) Differences in length, caused by the different length of the logs and by the variable edging necessary for removing faulty and tapered ends, are not essential to these considerations.

These boards, emerging from the saws in a random sequence (at a rate of about 1 per second at Domsjö Såg), must be sorted in types, not only with a view to their final delivery to the customer, but primarily in order to enable them to be *stacked* in regular fashion for the process of *drying*: only boards of one type can be combined to form a regular lattice, which is desirable for easy handling and controlled drying conditions in the hot-air chambers. Fortunately, the heavy heart planks need not be sorted since their width and thickness are fixed as long as logs of one diameter range are being sawn. All the thinner boards, after having been checked for visible defects, are transported by a single rapid belt conveyor (speed 210 m/min) to the sorting plant (*B* in the flow diagram of fig. 14).

Fig. 22. Electronic minimum-diameter gauge, installed at Skutskärsverken, Skutskär. In each of two arms A_1 and A_2, which form a letter V, a belt with a transverse slit runs along a series of 160 small lamps. The light of these lamps successively transmitted by the slit falls on a photocell mounted opposite each arm at a distance of 3.5 m (P_1; the other photocell cannot be seen) and produces a series of pulses. Fifteen pulse trains per second are produced by each arm and are fed to a counter with two registers, where they arrive alternately. A log which is passed between the two arms will screen a number of lamps from each photocell and thus decrease the number of pulses in each train. The number of pulses missing from these two trains is a measure of the thickness of the log in two directions at right angles to each other. Two consecutive pulse trains arriving at the counter are compared, the larger of them is stored in one of the registers and compared with the next pulse train appearing in the other register, and so on. The maximum thus found after the log has passed gives the minimum diameter. The accuracy is better than $\pm \frac{1}{4}$ inch. The gauge is provided with 22 relays giving output signals used for automatic sorting of the logs and for operating a display unit (*I*) which was used in the initial period after the installation of the equipment to provide a check on its operation.

Fig. 23. Board-sorting installation of Domsjö Såg. The planks are dropped from the large conveyor system on the left into the respective bays, where they are collected on trucks. A number of trucks which have already been filled and removed are seen at the right-hand side.

The most conspicuous part of the board-sorting plant at Domsjö Såg is a huge conveyor system 65 m long and 5 m wide, by which the boards are transported, in a direction perpendicular to their length, over a series of 30 bays; see *fig. 23* [8]). In this system each board is held by a suspension unit containing several hooks fixed on a spring-loaded shaft (*fig. 24*). The shaft carries three disks which can be slid along it to various positions. Above each bay is a release mechanism containing a lever, which is at a different position for each bay. When one of the disks of a suspension unit passing overhead hits this lever, the shaft of the suspension unit is released from its spring, so that the hooks will drop the board into a truck in the bay.

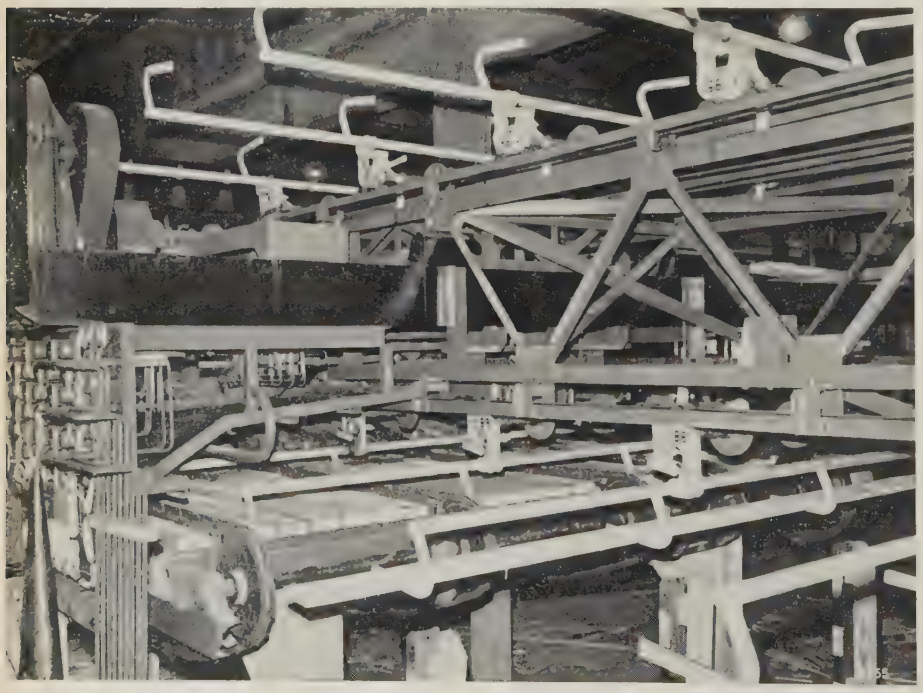

Fig. 24. First part of the conveyor system with suspension units. Unit 88 is carrying a board. On the upper side the units are returning to the starting point to the left in the photograph. The disks carried by each suspension unit and actuating the release mechanism of the respective bays are automatically shifted to the desired position by one of 30 relay units visible to the extreme left.

Now, the actual sorting is effected by equipment which automatically measures the width and thickness of each board arriving at the conveyor

[8]) The mechanical system was constructed by AB Nordströms Linbanor, the chief contractor for the board-sorting installation.

system and which, depending on these measurements, energizes one of 30 relay units. Each of the relay units controls a solenoid valve with a hydraulic ram in such a way that one of the disks of the simultaneously arriving suspension unit, which is going to take over the arriving board, is pushed to a coded active position [9]). (Just before this happens, the disks of this suspension unit are automatically reset to a zero position.) The functioning of this equipment can be explained in more detail with reference to *fig. 25*.

[9]) It would be difficult to make a ram long enough to shift a disk to any one of 30 different positions on the shaft. This is the reason why three disks are used, two of which remain in their zero position while the third is shifted to one of 10 active positions.

The *width* of the moving board is measured by means of a photocell arrangement which delivers a number of pulses proportional to the width of the board (20 pulses per inch). The pulses are fed to an active cold-cathode counter [10]) which, dependent on the number of pulses received, will give a positive pulse on one of 14 lines corresponding to 14 different widths varying from say 2 to 11″. At the same time the *thickness* of the board is measured by a simple mechanical gauge, which controls a stack of 14 three-way switches connected to the above-mentioned lines. The positive pulse is thus directed to one of 42

[10]) See e.g. F. Einramhof and P. Havas, Philips tech. Rev. **21**, 309, 1959/60.

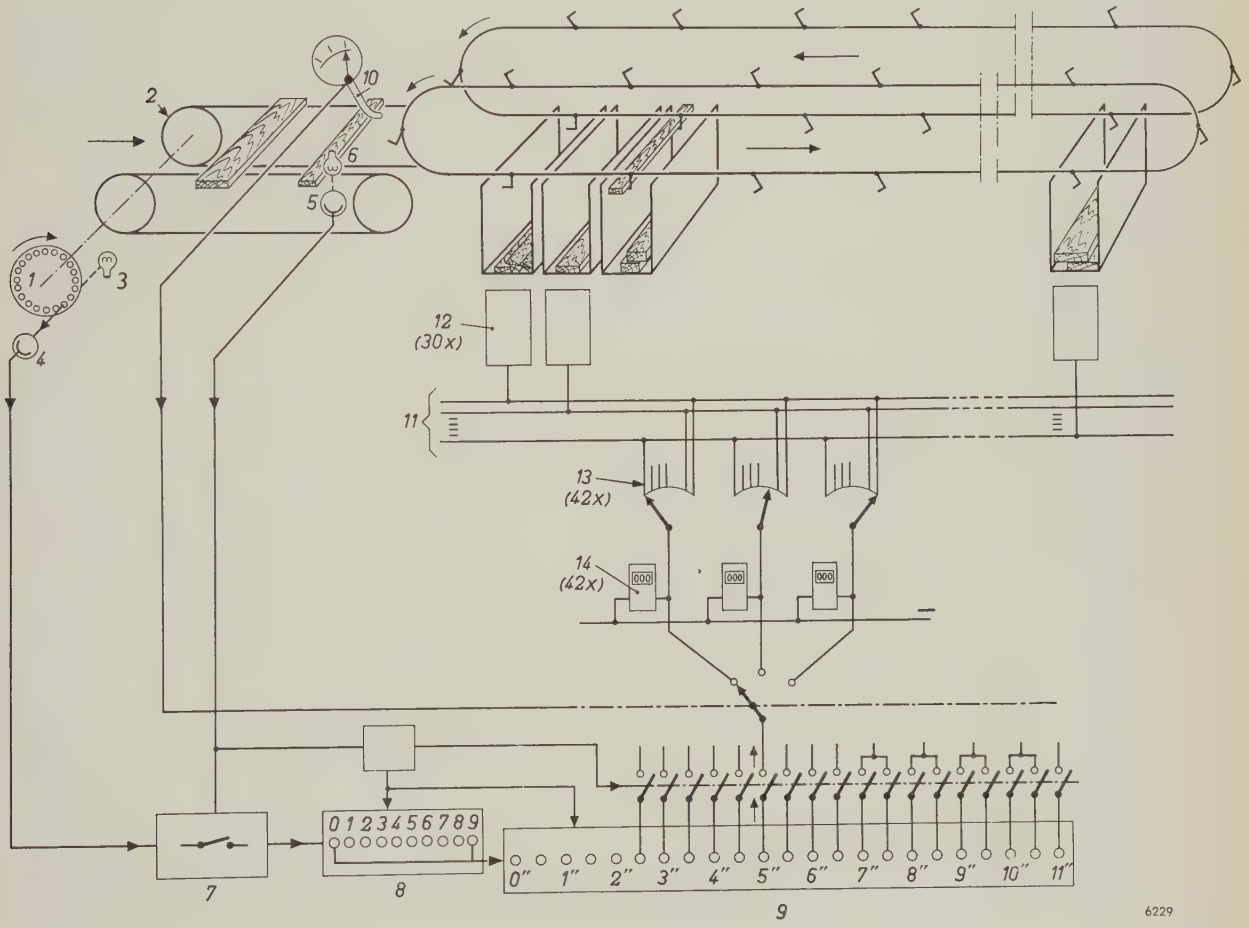

Fig. 25. Sketch of the board-sorting system. The perforated disk *1* is coupled to the conveyor *2* and produces a continuous series of pulses by interrupting the light of lamp *3* falling on photocell *4*. The number of pulses is directly proportional to the distance covered by the conveyor. A board arriving at photocell *5* will interrupt the light of lamp *6* and thereby open the gate circuit *7* where the aforementioned pulses arrive. The number of pulses transmitted by the gate is a measure of the width of the board — irrespective of the speed of the conveyor. After every ten pulses (corresponding to 0.5″), the active cold-cathode counter *8* will deliver a pulse to the shift register *9*, which has fourteen output lines. The reappearance of the light on photocell *5* will produce a signal closing the gate *7* and causing a positive pulse to appear on the last attained output line of *9*. This output line (which thus corresponds to the width range of the board being measured) is connected to one of three sub-outputs, selected by the mechanical thickness gauge *10*. Each of the 42 outputs thus available can be connected by means of a jack-and-cord switchboard *11* to one of the 30 relay units *12* which control the hydraulic setting of the disks on each suspension unit. Each output is also provided with a selector *13* bypassing the switchboard. The selector is actuated by a negative pulse from the corresponding preset counter *14* for selecting a free relay unit when a bay has been filled.

outputs, arranged on a switchboard. Each of these 42 outputs can be connected to each of the 30 relay units by a jack and cord (*fig. 26*).

In reality, not more than 8 width classes (24 types of boards) are to be expected on a given day, as explained before. Only 24 outputs will therefore actually be used at one time.

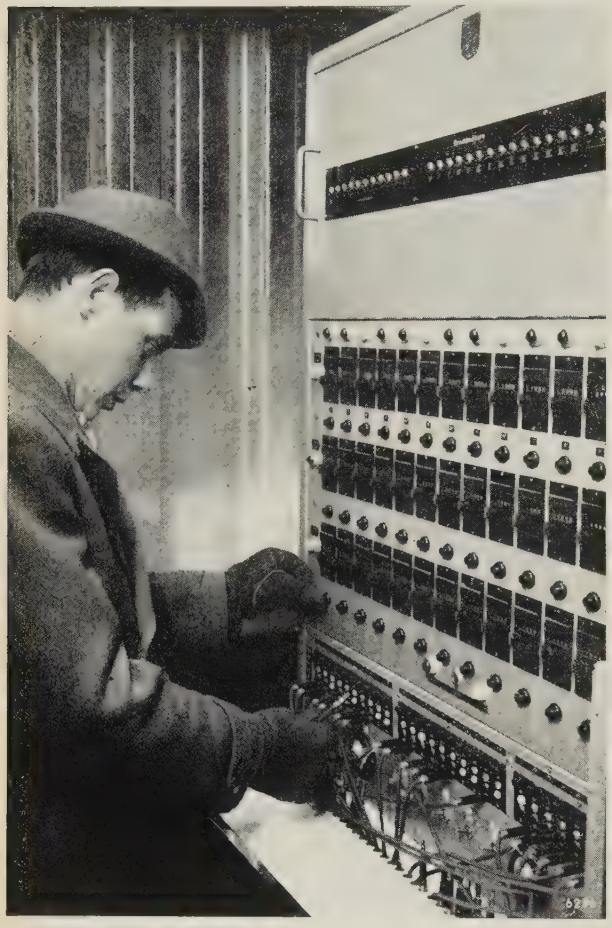

Fig. 26. Cabinet with 42 outputs (below) of the device for measuring the width and thickness of the boards. Each output can be connected by jack-and-cord with each of the 30 relay units for the 30 bays (no more than 24 types of boards will occur during one shift owing to the established sawing strategy). Above these inputs with their signalling lamps are the 42 preset counters for the automatic selection of a free relay unit when one of the bays has been filled.

When the truck of a bay has been filled to capacity, the bay must be put out of use until the personnel have emptied the bay and put another truck in it. To prevent difficulties arising from bays being filled too high, an automatic changing system has been provided. Each of the 42 outputs on the switchboard is provided with an electro-mechanical counter, which can be preset to the number of boards of the pertaining type that can be collected in one bay. When this preset number is reached the counter will deliver a negative pulse which starts a rotary 30-step switch (cf. fig. 25) automatically selecting a relay unit (i.e. a bay) not being used at the moment. The following boards of this type thus will be discharged into the new bay. At the same time the counter is automatically reset to zero, a lamp is lit on the switchboard to indicate the relay unit now occupied and another lamp is lit at the bay which has been filled, warning the personnel to empty the bay.

Emptying a bay will take some time and other bays may become filled in the meantime. It is, however, unlikely that more than 4 or 5 bays will be waiting to be emptied at any given moment. Thus, 30 bays (30 relay units) are sufficient for the 24 different types of boards.

The board-sorting installation can be operated manually, in the eventuality that the electronic equipment should fail. This precaution was necessary in order to ensure the continuous flow of logs and boards through the plant under all circumstances. No use has had to be made of this facility at Domsjö Såg so far.

Let us now have a closer look at the changes brought about in the production process by the application of electronics. Log sorting in accordance with the sawing strategy used to be done, in a cruder form and manually, before electronic means were available. Electronics is saving labour and improving accuracy here too, but as in the other cases other very important advantages are also obtained. In the manual process of sorting, the floating logs were grouped by simply pushing them to the desired bay, and the available water surface was exhausted when it was covered by a layer one log thick. In the modern process, the logs are collected in bundles of 100-300 which are tied together, covering the water with a layer several logs thick, on the average. Many more logs of each class can thus be kept in the storage space of a given harbour basin. This saving of storage costs is similar to that found in the shoe-last factory, but that is not all. The possibility of feeding one single class of logs to all the sawing lines during at least one shift ensures that not more than 24 types of boards will come out of the saws during this period. Had this not been so, the very large and expensive board-sorting plant would have needed more than 50 bays instead of 30, in order to cope with all the 42 possible types of boards at the same time. The enormous hall and mechanical conveyor system necessary for this number of bays would have more than doubled the investment costs for this operation.

Tying the logs together in bundles, rendered possible by the sorting process described above, can bring another unexpected advantage. Logs lose a large part of their buoyancy when debarked, so much so that with some types of trees 20% of the logs will sink after some time and disappear to the bottom of the harbour basin. These logs ("sleepers") have to be regained by regular dredging operations and fitted with floating planks of light wood in order to bring them to the conveyors for the saws. When tied together, however, the logs still capable of floating — 80% of the total — will keep the other ones afloat too, and no difficulty is experienced in bringing the whole bundles to the saws. Logs that sink when a bundle is untied can easily be spotted and put directly on the conveyor.

The applications of electronics described in this article will have made it clear that the potentialities of electronics are well appreciated and widely used in the wood industry. There is no doubt that more and wider applications in this field will be found, especially in Sweden, where close collaboration between the wood industry and the electronic industries is now firmly established.

Summary. Description of a series of relatively new applications of electronics in the Swedish wood industry, with emphasis on the character of the changes effected in manufacturing processes. High-frequency gluing is mentioned only in passing, since this has been common practice for a number of years. High-frequency drying introduced in a factory making shoe lasts at Järrestad has reduced storage costs to 15% of their former value and at the same time diminished the rejection rate because of cracks from 8-10% to 1-2%. In a match factory at Vetlanda, strips of veneer for match boxes are inspected for defects at a rate of 400 strips per minute by a photoelectric scanning device, reducing the manual labour involved in the total manufacturing process by 10%. A similar photoelectric device developed for sorting oak parquet blocks into four categories in a factory at Ronneby has resulted in a notable improvement of the quality of the product, in addition to saving labour. The important role electronics is beginning to assume in large sawmills is discussed at some length. A log-sorting plant for 3400 logs daily and a board-sorting plant for 10 times this number of boards, both in use in a sawmill at Örnsköldsvik for the past few years, are described and brief mention is made of a metal detector and an automatic minimum-diameter gauge for logs. Saving of labour and storage costs are again the chief advantages obtained, in addition to simplifications in the production process.

A SNOW SEPARATOR FOR LIQUID-AIR INSTALLATIONS

by C. J. M. van der LAAN *) and K. ROOZENDAAL *).

533.24:66.078

The time during which a gas refrigerating machine can continuously produce liquid air is limited by the gradual blockage of the separator in which the gaseous impurities removed from the air feed settle in the form of ice or snow. The old form of separator had to be defrosted after every 120 litres of liquid air produced, i.e. every twenty-four hours when the machine was in continuous operation. With the new design described below, which is quite different from all known designs, defrosting is necessary only after 600 litres of liquid air have been produced.

Before air is liquefied, it must be freed from impurities such as water vapour and carbon dioxide, otherwise the equipment would soon be blocked up by ice and solid carbon dioxide.

Water vapour and carbon dioxide can be removed by the use of chemicals such as silica gel or potassium hydroxide. This method has drawbacks, however: potassium hydroxide is a corrosive substance and very unpleasant to use; silica gel has to be regenerated from time to time, which complicates the installation, and moreover under tropical conditions a large drying plant is needed. A smaller drying plant might be sufficient if the air were compressed, but the use of a compressor is in itself an added complication. It consumes electrical energy, calls for maintenance, and must be of a special type in which the air is not contaminated by lubricants.

The Philips gas refrigerating machine [1]) was therefore designed right from the start to freeze out the impurities before the air is liquefied. This was formerly done in an "ice separator" (*fig. 1*), consisting of horizontal perforated copper plates kept cold by the

*) Industrial Equipment Division, Eindhoven.

[1]) J. W. L. Köhler and C. O. Jonkers, Fundamentals of the gas refrigerating machine, and Construction of a gas refrigerating machine, Philips tech. Rev. **16**, 69-78 and 105-115, 1954/55.

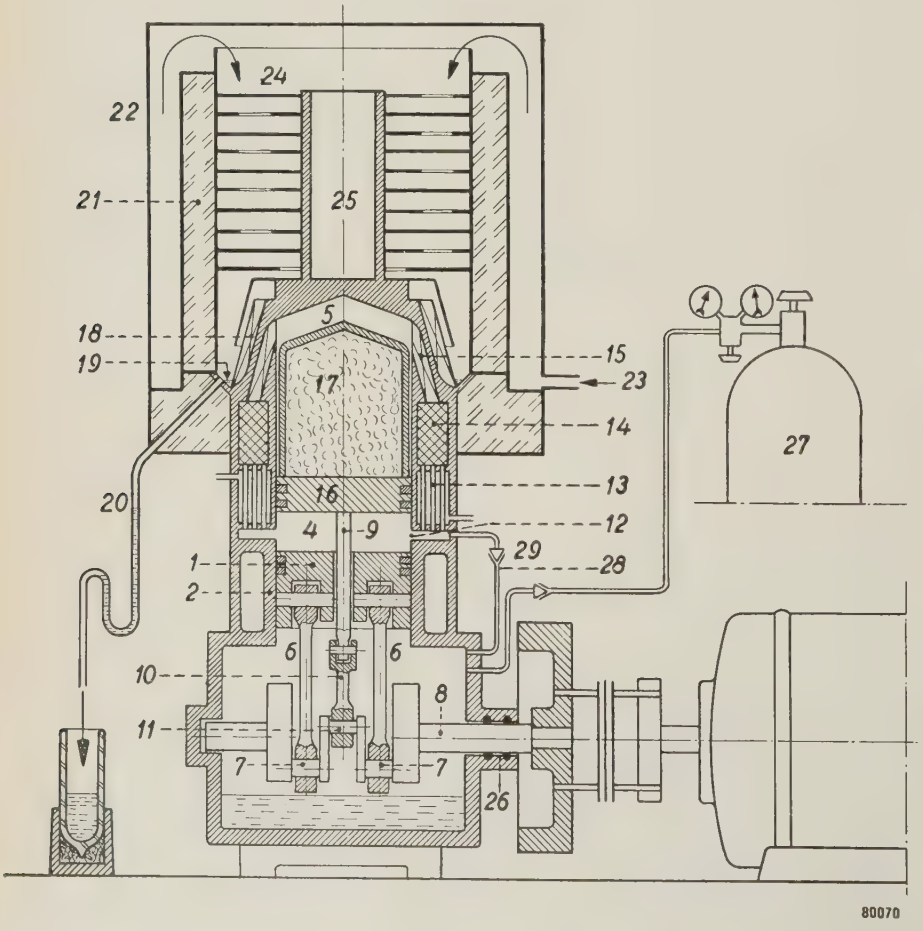

Fig. 1. Simplified cross-section of a gas refrigerating machine for producing liquid air [1]), illustrating the ice separator consisting of perforated copper plates *24*. The plates are in contact with the head ("freezer") *15* of the refrigerating machine via the tubular structure *25*. The air enters at *23* under atmospheric pressure, flows along the plates *24* where moisture and carbon dioxide are removed, is liquefied on the condenser *18*, and is tapped off via the annular channel *19* and the delivery pipe *20*. *21* is an insulating wall, *22* the jacket around the ice separator.

The significance of the other figures is: *1* main piston, *2* cylinder, *4* and *5* spaces between which the gas flows to and fro, *6* connecting rods, *7* cranks, *8* crankshaft, *9* displacer rod with connecting rod *10* and crank *11*, *12* ports, *13* cooler, *14* regenerator, *16* piston and *17* cap of the displacer, *26* gas-tight shaft seal, *27* gas cylinder supplying refrigerant, *28* supply pipe, *29* one-way valve.

machine itself. The moisture and carbon dioxide in the air formed deposits of ice or snow on these plates, and the purified air passed through the holes.

The great drawback of this type of separator is that it soon becomes clogged up, owing to the ice and snow settling principally on only one or two of the plates. This is due to the fact that the moisture content of saturated air decreases very rapidly as the temperature drops (*fig. 2*). Nearly all the moisture therefore settles on those plates whose temperature is only slightly below 0 °C. The already dry air is then further cooled by the following,

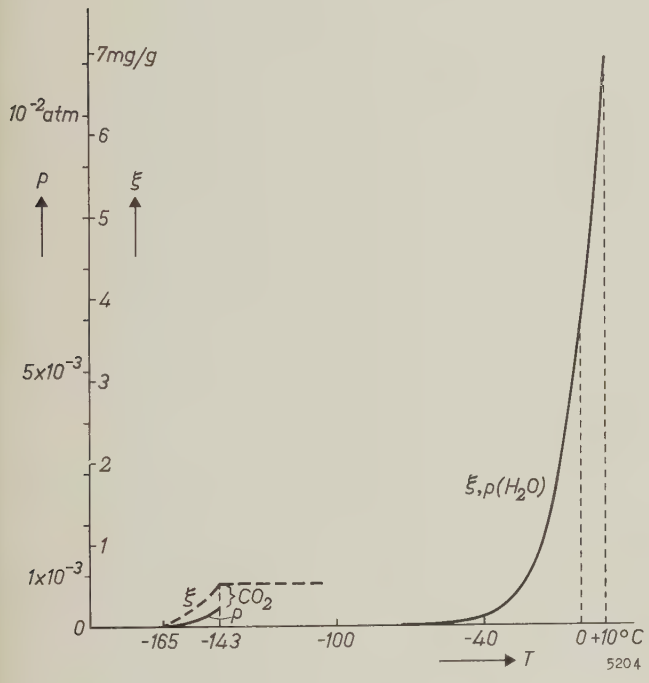

Fig. 2. Water-vapour and carbon-dioxide content ξ and their vapour pressure p in saturated air as a function of temperature T (ξ is expressed in milligrams of water vapour or carbon dioxide per gram of dry air).

colder plates, but the spaces between them are no longer filled with snow, except at the last, very cold plates, where carbon-dioxide snow is formed. In spite of the 14-litre capacity of this ice separator, about 1 kg of snow and ice is enough to cause a blockage. A machine fitted with such a separator is therefore unable to produce more than 120 litres of liquid air before it has to be stopped for defrosting.

Efforts to improve on this performance have resulted in a new design, which will be discussed below. The new separator traps the water vapour of the air only in the form of snow, hence its name.

The snow separator

The design of the new separator is based on a surprising fact which was discovered by chance by the authors in an investigation directed towards another end [2]). It was found that when a stream of air is passed through a gauze kept at a very low temperature the layer of snow formed on the gauze remains porous for a considerable time. At first sight one would expect that the layer of snow would quickly grow into a compact mass, but in fact the crystals form in such a way that this is not so.

In the new separator, whose size is no greater than that of the former type (14 litres), this phenomenon has been turned to practical use so that about 5 kg of snow can be stored without causing a blockage. This means that the machine can produce five times as much liquid air in continuous operation. Whereas the old type of separator had to be defrosted every day, once or twice a week is now sufficient.

The principal component of the snow separator is a cylinder of fine copper gauze (*fig. 3*) kept at low temperature in a manner presently to be discussed. This "snow gauze" is surrounded by a double jacket (the snow forms in the space between the jacket and the gauze). The air feed flows via the double jacket, in which it is precooled, to the snow space, passes through the gauze and is then condensed on the head of the refrigerating machine. As the air flows through the gauze, a layer of snow forms on its surface. The layer progressively thickens into a snow cap, through which the air still has to pass. A "snow cake" from which a piece has been removed is shown in *fig. 4*. This cake took a week to grow to a thickness of about 10 cm; the innermost layer, about 0.5 cm thick, consists of carbon-dioxide snow. The density of the snow is fairly high, the values measured being 0.4 g/cm^3 for the water snow and 0.9 g/cm^3 for the carbon-dioxide snow. Nevertheless, the layer is still porous, and the pressure drop across it when the machine is working at full capacity is no more than 20 cm water column.

What are the conditions to be fulfilled in order to keep the snow layer porous? To answer this question we must have a clear picture of the way in which the layer of snow is formed.

Formation of the snow layer

As long as no snow has yet formed on its surface, relatively warm air enters into contact with the gauze. To prevent the transport of the fairly large amount of moisture still present in the air feed, the gauze must be capable of cooling the air to a very low temperature. First of all, then, the gauze itself must be kept at the very low temperature

[2]) Dutch Patent No. 98 130.

of —165 °C (the temperature of liquid air is —194 °C). Secondly, to provide good thermal contact with the air, the gauze must have a fine mesh.

Once the machine is started, part of the impurities will initially settle on the gauze by diffusion, i.e. through the movement of water vapour and carbon dioxide caused by local differences in partial vapour pressure. At the surface of the cold gauze the partial vapour pressures are much lower than in the warmer air feed (fig. 2). As a result, the layer of snow grows counter to the direction of air flow. very porous layer, with long needles, has meanwhile formed on the outside; this absorbs the major part of the following small crystals, thus preventing any stoppage of the first layer for a considerable time, and so the process goes on. Conditions must therefore be chosen in such a way that the snow settles mainly on the outside of the layer, thus minimizing the quantity of impurities that can settle inside.

Since the mass of an impurity transported per second is proportional to the partial pressure of

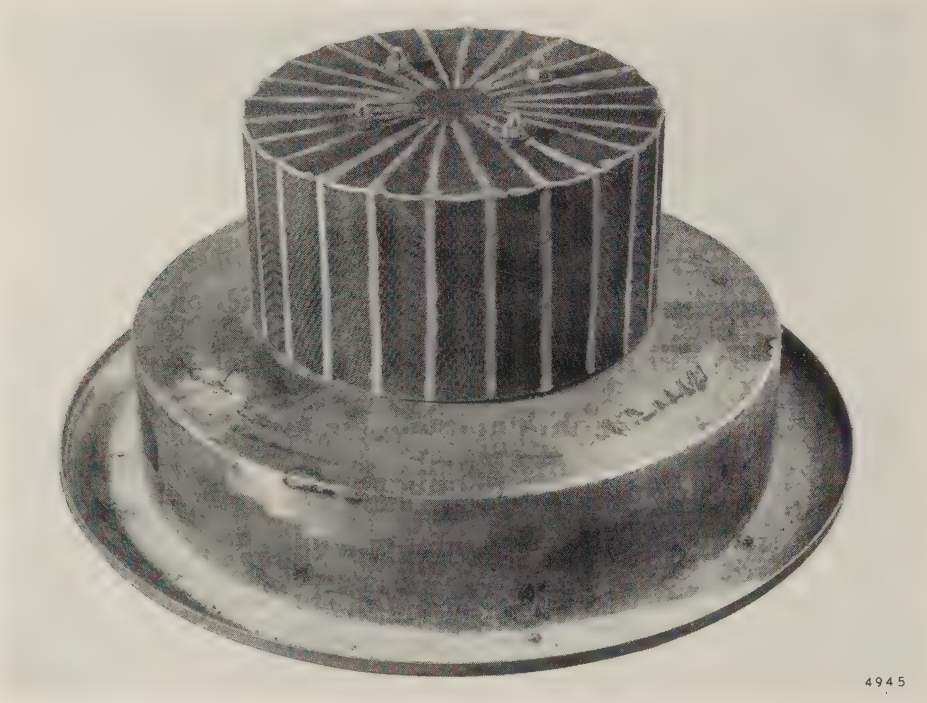

Fig. 3. Cylinder of fine copper gauze, on which water vapour and carbon dioxide from the air are deposited in the form of porous snow.

In the beginning a small proportion of the impurities forms snow crystals in the air stream itself and passes through the gauze. This is unavoidable. The rest, however, settles on the gauze and increases the heat-transfer surface area, forming a thin layer of snow pierced by numerous narrow channels. Both the heat transfer and the deposition of impurities are virtually 100% effective as soon as this thin layer is formed.

The snow first settles in the form of relatively long needles. The space between the needles is then gradually filled up with smaller snow crystals. As long as the temperature of the snow layer remains far enough below the melting point, no ice forms. Although the accumulation of smaller crystals decreases the porosity of the first layer, a fresh and that impurity in the air, steps must be taken to ensure that the temperatures in the snow layer are such that the partial pressure therein (i.e. the vapour pressure corresponding to the local temperature) is much lower than the partial pressure in the air feed. To meet this requirement, the temperature everywhere in the snow layer must be kept below a specific value, since the vapour pressure drops sharply with decreasing temperature (see fig. 2). Experiments have shown that the temperature of the outside of the water-snow layer must remain below —40 °C if the dew point of the incoming air is 10 °C. Since the outside layer is heated by the incoming air, the layer must be kept at this low temperature by conduction via the snow crystals to the cooled gauze.

Fig. 4. A porous snow cake, about 10 cm thick, grown on the gauze in about a week.

Where the surface temperature of the snow layer is —40 °C, 99% of the moisture in the air feed will settle on the outside, and only 1% will enter the layer as vapour and form snow further inside where the temperature is lower (see fig. 2). Where the temperature inside the layer is lower than —143 °C, the carbon dioxide also forms snow. In order to ensure adequate trapping of the carbon dioxide, the temperature of the gauze should not exceed —165 °C. At this temperature 1% of the carbon dioxide in the air feed is still transmitted; this has been found to be a tolerable percentage.

With the first designs of the snow separator, the moment at which the machine had to be stopped for defrosting because of excessive resistance to air flow was determined by the amount of carbon dioxide in the layer of water snow. An important improvement was later introduced by surrounding the cylindrical snow gauze (fig. 1) with a layer of metal gauze folded in zigzag form roughly 12 mm thick (*fig. 5*). The water snow then forms on the outside of this "concertina gauze", whilst the carbon-dioxide snow has ample space to settle inside it. This substantially postpones the moment at which the resistance to flow becomes excessive.

In the foregoing we have referred to *the* temperature of the snow gauze, as if this temperature were everywhere the same. This is not so, however. Heat is supplied to the gauze over its entire surface, and must flow by conduction through the wires to the places where the gauze is brazed to cooled strips or pipes (these structural details are indicated in the figures at the end of the article). Midway between the brazed joints the gauze is therefore not so cold. Evidently, the temperature differences in the gauze must be small if the temperature at all points is to be kept below —165 °C, in other words the gauze must be a good heat conductor. Simple calculations and experiments have shown that the only suitable material for the gauze is copper wire, which must not be too fine.

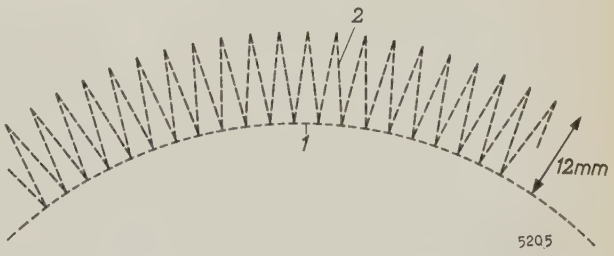

Fig. 5. A layer of "concertina gauze" *2*, about 12 mm thick, is fitted around the snow gauze *1*. This promotes the deposition of water snow on the outside of the layer, and offers more space for carbon-dioxide snow to settle.

Another initial difficulty was that if the air feed entered the snow space through a small aperture, and thus at such a high velocity that turbulences arose, the snow layer very soon became impenetrably dense. We can explain this as follows. The eddying air is strongly cooled by the surface of the snow, giving rise to hard snow crystals that show no tendency to settle to form the porous layer required. Snow of this structure, called "polar snow", evidently fills up the fine channels completely, causing a sharp increase in the air-flow resistance. If the air is allowed to enter the snow space through a large aperture, and thus at lower velocity, no difficulties are experienced. Although the large temperature differences existing might be expected to cause convection currents in the air, these currents (if they exist) are not troublesome.

The thermodynamics of the snow separator

We shall now consider the thermodynamics of the snow separator, with special reference to the magnitude of the air flow which can be handled. For this purpose we make the following simplifying assumptions.

1) The temperature of the air and that of the snow are everywhere equal, i.e. there is infinitely good thermal contact.
2) The entire latent heat of sublimation of the impurities and the heat absorbed while cooling the air feed to the temperature of the outer surface of the snow layer are released at the surface (in reality this heat is released in a layer a few millimetres thick).
3) Since, in accordance with assumption (2), the latent heat of sublimation of the small quantity of impurities deposited *in* the snow layer is disregarded, the enthalpy H of the air inside the layer must be a linear function of the temperature T. The rate of change of the enthalpy with temperature is equal to the specific heat c_p of air at constant pressure:

$$\frac{dH}{dT} = c_p . \quad \ldots\ldots \quad (1)$$

The variation of the enthalpy H of the air with temperature T is shown in *fig. 6*. (Since the enthalpy of a gas is determined but for an additive constant, which we can choose at our convenience, we are at liberty to assume the enthalpy of the air feed (at 10 °C, 1 atm) to be zero. This simplifies the calculations given below.)
4) The thermal conductivity λ of the snow is assumed to be identical and constant at all points (in reality λ depends on the temperature and density of the snow, and also on its structure).
5) Although the snow gauze and the outside of the cake of snow have the form of coaxial cylinders, we shall regard them as parallel flat surfaces. A cylindrical section through the snow layer at a distance x from the gauze then becomes a flat surface whose area A in fact depends on x. We will assume however that this area is constant and equal to the average of the surface area of the gauze and that of the cake of snow.

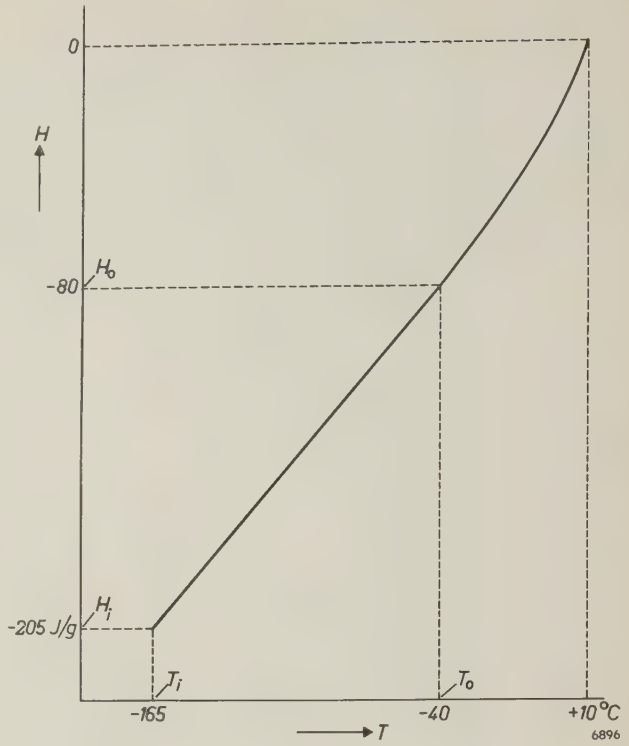

Fig. 6. Enthalpy H of air as a function of temperature T. The enthalpy of the ambient air is assumed to be zero.

In the steady state, the total heat flow through every cross-section of the layer is constant. It may easily be shown that it follows from assumption (3) that the magnitude of this heat flow is in fact zero. (This brings out the rather artificial nature of assumption (3), since one normally regards the heat content of a body as being positive, but this in no way detracts from the validity and utility of the assumption.) The total heat flow consists of an enthalpy flow in the air and a heat flow conducted by the snow. The enthalpy flow is equal to mH, where m is the mass of air displaced per second, and the heat flow through the snow is equal to $-\lambda A dT/dx$. We may therefore write:

$$mH - \lambda A \frac{dT}{dx} = 0 .$$

Subject to the assumptions mentioned above, this equation defines the variation of the temperature of the air with the distance x from the snow gauze as shown in *fig.* 7. Making use of eq. (1), and integrating over the layer thickness x_0, we find:

$$-\frac{m\, c_p x_o}{\lambda A} = \ln \frac{H_i}{H_o}, \qquad \ldots\ldots (2)$$

where the subscripts i and o relate to the inside and outside of the layer respectively.

For the reasons already discussed, we put the temperature T_i of the gauze at —165 °C and the maximum permissible temperature T_o of the surface at —40 °C; it may be seen from fig. 6 that the corresponding enthalpy values are then $H_o = -205$ joules/gram and $H_o = -80$ joules/gram. In the design adopted the maximum thickness x_o of the snow was 7 cm and the average cross-sectional area A was 0.2 m². Given $c_p = 1$ joule/gram°C and $\lambda = 0.6$ W/m°C, we find from (2) that the maximum permissible air flow is $m = -1.6$ grams per second. (The minus sign indicates that the air flow is in the negative x direction, as shown in fig 7.) This is in reasonable agreement with the value of 1.8 grams per second found in practical operation.

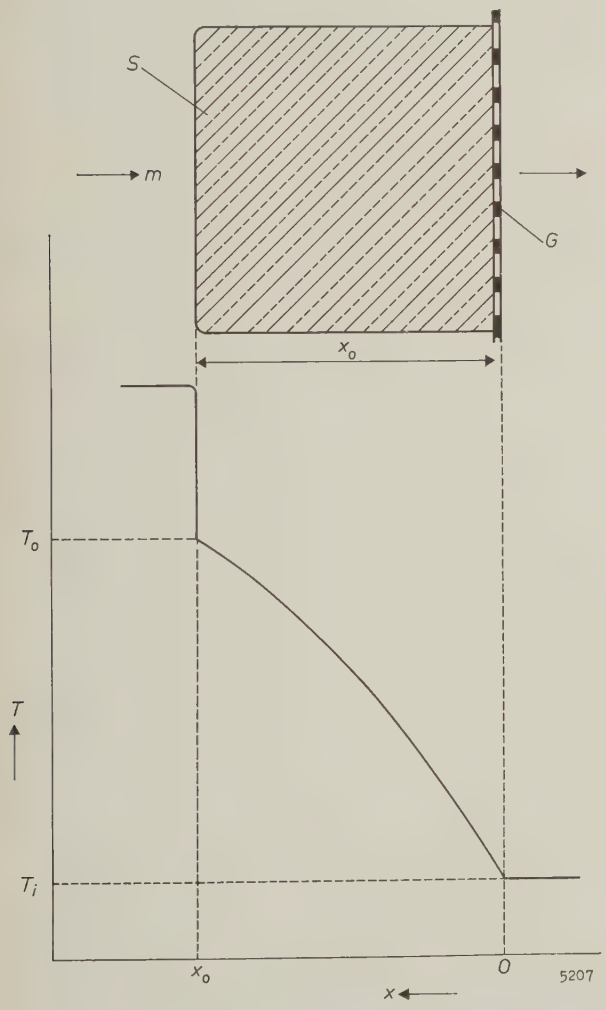

Fig. 7. Above: axial cross-section through the snow cake S, of thickness x_o. The snow gauze is denoted by G, the air flow by m. (Since the air flow is in the negative x direction, the value of m will also be negative.)
Below: variation of temperature T with distance x from the snow gauze.

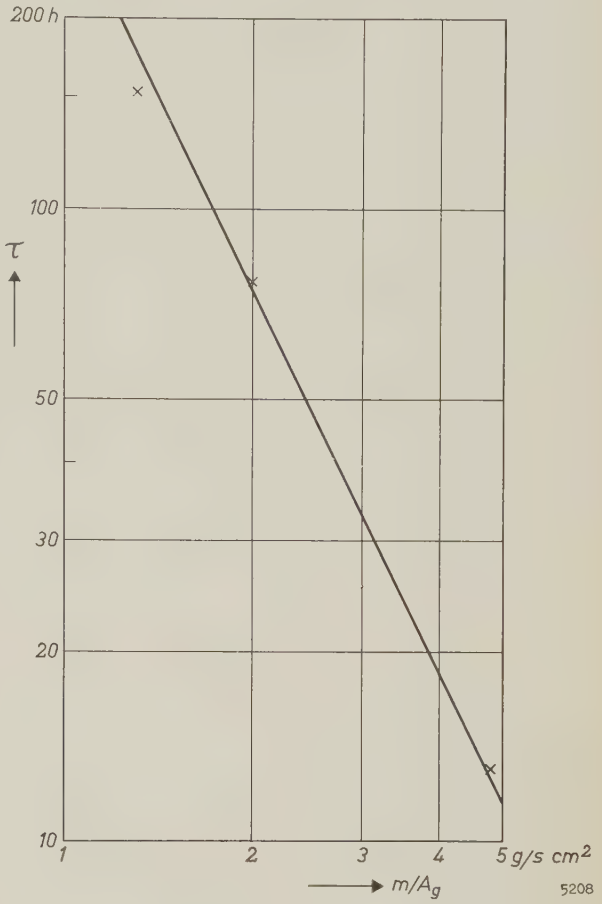

Fig. 8. "Operating time" τ as a function of air flow m per unit surface area A_g of the gauze. The straight line represents the relation $\tau \propto m^{-2}$; the crosses relate to measured values.

If the moisture content is 0.75% by weight (dew point 10 °C) and the density of the snow is 0.4 g/cm³, it follows that the "operating time" is 4½ days (i.e. the machine can run continuously for 4½ days before defrosting). If the air flow is twice as large, so that twice the amount of impurities is supplied per second, we see from (2) that the thickness x_o at which the temperature has risen to the point where the separator no longer works efficiently (—40 °C) is then halved, and so too therefore is the snow storage capacity. The operating time τ is consequently four times shorter. This quadratic effect ($\tau \propto m^{-2}$) is in fact found in practice (*fig.* 8).

It also appears from (2) that it must be advantageous to increase the thermal conductivity λ, for example by introducing copper pins or strips in the

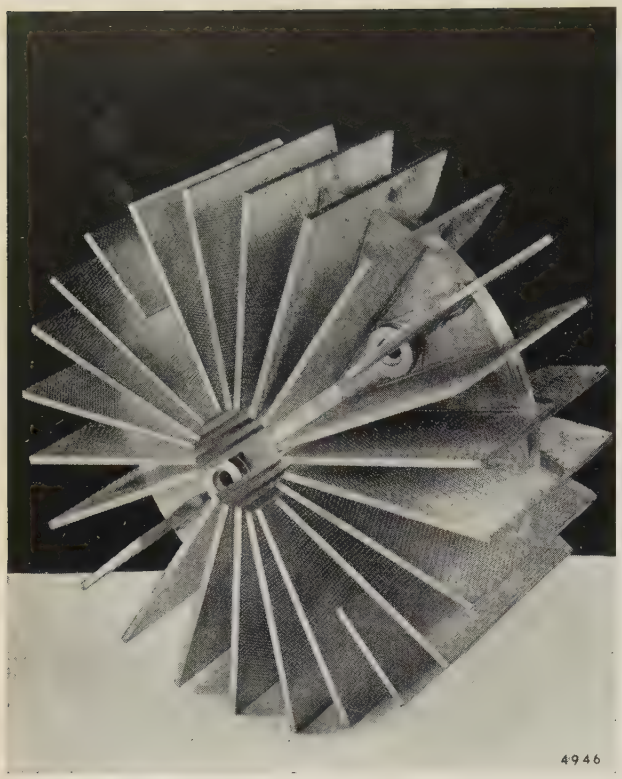

Fig. 9

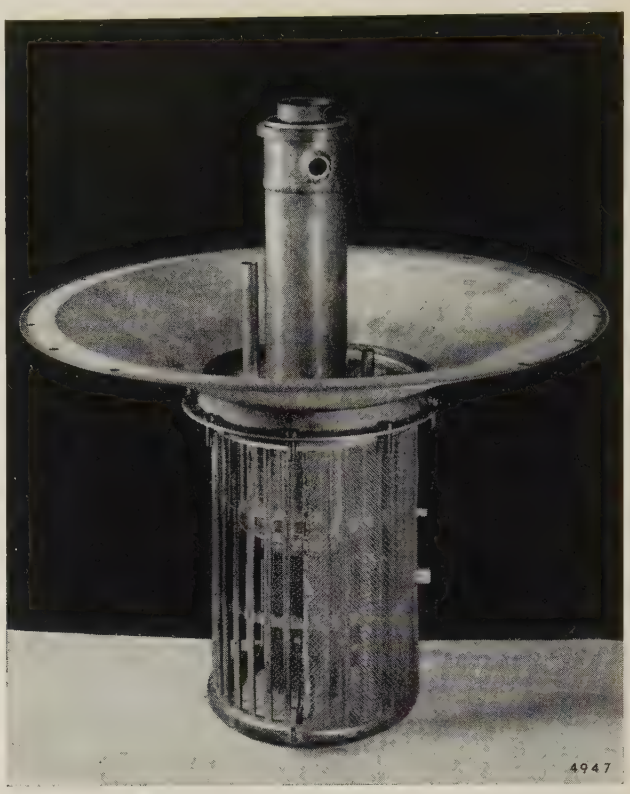

Fig. 10

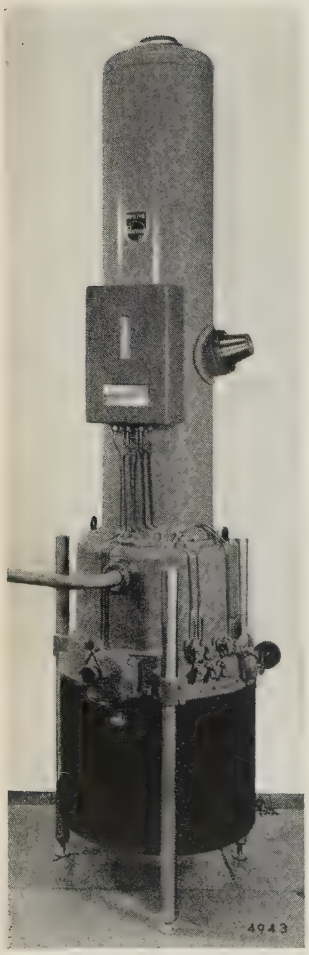

Fig. 11

Fig. 9. In the gas refrigerating machine the snow gauze is brazed to the radial copper grid illustrated here, which is bolted to the cold head of the machine and thence dissipates the heat directly.

Fig. 10. In air-fractionating installations for producing liquid nitrogen, the snow gauze (here partly removed) is brazed to a crown of copper pipes, through which liquid oxygen of about –180 °C flows.

Fig. 11. Air-fractionating column (without refrigerating machine) for supplying liquid nitrogen [3]). The bottom, dark section is an insulating jacket. in which the structure shown in fig. 10 is located.

snow. The concertina gauze mentioned above also works along these lines.

Finally, the snow separator as used in a liquid-air machine and in an air-fractionating column [3]) is illustrated in *fig. 9*, *10* and *11*. Various structural details are mentioned in the captions.

[3]) J. van der Ster and J. W. L. Köhler, A small air fractionating column used with a gas refrigerating machine for producing liquid nitrogen, Philips tech. Rev. **20**, 177-187, 1958/59.
J. van der Ster, The production of liquid nitrogen from atmospheric air using a gas refrigerating machine, thesis, Delft 1960.

Summary. Before liquefying air, it is necessary to remove the moisture and carbon dioxide it contains. Until recently, the Philips gas refrigerating machine used a separator on which these impurities settled in the form of ice and snow. A drawback of this separator was that it had to be defrosted once a day. An entirely new design of separator is discussed here, consisting of a cylindrical jacket of copper gauze, which is kept at a temperature of –165 °C and through which the air feed is passed. Water vapour and carbon dioxide settle on the gauze as a layer of porous snow (hence the name "snow separator"). The layer remains porous for days and causes no appreciable pressure drop. Defrosting is necessary only after a continuous production of 600 litres of liquid air (five times as much as before), i.e. once or twice a week. The snow separator is also being used with advantage in air-fractionating systems.

DOSEMETERS FOR X-RADIATION

by J. HESSELINK *) and K. REINSMA *).

621.386.82:615.849.5-015.3

In recent years the conviction has gained ground that dosimetry should no longer be limited to X-ray therapy, but should be extended to the small doses administered in X-ray examinations. In the article below, after a discussion of dosemeters for use in X-ray therapy, an easily operated instrument for determining diagnostic doses is described. This instrument, unlike therapy dosemeters, measures the total energy incident on the patient. It can help radiologists in their efforts to use X-radiation sparingly.

Introduction

If proper use is to be made of X-rays in medicine, it is necessary to know with reasonable accuracy the amount of radiation administered to the patient. In therapeutic treatments this applies first and foremost to the doses received by patients individually; the optimum effective dose here is sometimes not much smaller than the maximum permissible dose, and in such cases the margin of uncertainty must be no more than 3 to 5%. In diagnostics we are mainly concerned with the amount of radiation received by the population as a whole. Although the diagnostic dose given to each patient at a time is generally small, X-ray examinations as a method of diagnosis are used on a very wide scale in the more advanced countries. No less than 75 to 90% of the total quantity of medically administered radiation reaching the sex glands of the inhabitants of these countries (the gonad dose) is due to X-ray examinations. In some of these countries this amount is roughly equal to that from natural sources (cosmic radiation, radioactivity of the soil and building materials, K^{40} and C^{14} in the human body, etc.) so that caution is obviously called for. The conviction is growing that even the small diagnostic doses received by the sex glands may, in their cumulative effect, be genetically harmful to the population. In view of the increasing use of X-radiation for diagnostic purposes it therefore seems desirable not to limit dose measurements to therapeutic treatments. The regular measurement of diagnostic doses will enable the radiologist to make more sparing use of X-rays, and may lead to the development of new equipment with which the radiologist can obtain more information with a smaller dose [1]).

The physical quantity with which the biological effect of radiation can best be correlated is now generally held to be the *energy absorbed by the patient* [2]). Since there is no way of measuring that energy directly, an attempt has to be made to derive its magnitude from the measurement of some physical or chemical effect brought about by the radiation.

In the course of the years many and various dosimetric methods and instruments have been developed and put to use. We may mention the photographic plate, the ionization chamber, the Geiger-Müller counter, the proportional counter and the scintillation counter; new prospects are offered by the conversion of ferrous ions into ferric ions in a suitable iron compound, the colouring of certain types of glass and the change in the resistance of cadmium sulphide upon irradiation. In this article, however, we shall be solely concerned with instruments whose operation is based on the ionization produced by X-rays in passing through a gas — in our case air — and which measure the charge carried by the ions thus formed. Such an instrument consists essentially of a gas-filled space containing two electrodes connected to a measuring device.

To measure the charge produced by ionization per unit time, a potential difference is applied between the electrodes and the current flowing in the circuit is measured. This allows the determination of the dose rate at the site of the chamber. The total dose is found from this by integrating the current with respect to the time of exposure. The integration may be carried out by the circuit itself, simply by incorporating a capacitor in it. After the irradiation it is then simply a matter of measuring the potential to which the condenser has been charged by the ion current. The gas-filled space referred to, which functions as a radiation detector, is in both cases called an *ionization chamber*.

For measurements at many places at the same time, without the need for separate measuring

*) X-ray and Medical Apparatus Division, Eindhoven.

[1]) Report of the United Nations Scientific Committee: "On the effects of atomic radiation", Ch. 3, New York 1958.

[2]) Recommendations of the International Commission on Radiological Units (I.C.R.U.) 1950. See Brit. J. Radiol. **24**, 54, 1951.

equipment for each chamber, use is made of *condenser chambers*. These work on the same principle as the ionization chamber, but they are not attached to the measuring equipment during irradiation. The chamber is first charged to a certain voltage. It is then removed for exposure to the radiation, and returned to the measuring equipment for reading the decrease in voltage. A condenser chamber is therefore in fact a charged capacitor with a gaseous dielectric, which is partly discharged during irradiation. Obviously, the condenser chamber only measures doses and not dose rates, although the average dose rate can simply be found by dividing the dose reading by the exposure time.

In this article we shall discuss examples of both types of instrument: ionization chambers for use in radiotherapy, condenser chambers for various purposes, and finally a special type of ionization chamber for diagnostic use.

The question now arises as to what relation exists between the energy which an irradiated patient absorbs — either totally or in a specific part of the body — and the ionization which the same radiation causes in the same period of time at the same place in free air. Unfortunately the relation is not always a simple one. We shall therefore consider briefly the physical factors that govern this relation, after first giving the definitions of two concepts of dose in current use and the units in which these doses are expressed.

Dose definitions and units; physical principles of dosimetry

The oldest dose specification still in common use, and now called the exposure dose, is based on the ionization which the radiation produces in air. The unit of exposure dose is the roentgen, defined as "an exposure dose of X- or γ-radiation such that the associated corpuscular radiation per 0.001293 grams of air produces, in air, ions carrying 1 electrostatic unit of quantity of electricity of either sign" [3]).

Two points should be noted in this connection. As mentioned, the relation between the exposure dose just defined and the energy absorbed by the patient is not always simple. The continued use of ionization as a direct measure of dose is due to the fact that the ionization can readily be measured and conveniently used for charting a radiation field (for determining isodose curves, etc.). Further, it was discovered in the early days of radiology that a close relation existed between the exposure dose and the biological effect of the rays on muscular tissue, for the types of X-rays then most commonly used.

Secondly, some remarks on the words: "the associated corpuscular radiation per 0.001293 grams of air". The ionization of the air produced directly by the X-ray quanta is negligible compared to that produced by the electrons which the quanta eject from the atoms in their path. These (secondary) electrons acquire the whole of the energy of the quanta in question (photoelectric effect), or a part of it (Compton effect), as kinetic energy, which they in turn lose by collision with other atoms or molecules, giving rise to excitation or ionization. Such electrons produce in air an average of one ion pair for every 34 eV of kinetic energy they possess, so that an X-ray quantum of energy 50 keV would produce about 1500 ion pairs, only one or two of them directly. The exposure dose as defined above is therefore not identical with the ionization produced in the volume occupied by 0.001293 g of air (which is exactly one cubic centimetre at 0 °C and 76 cm Hg), but with the ionization produced by the secondary electrons released in that volume. This makes no difference in a large space uniformly irradiated with X-rays, but it does in a small enclosed space. We shall return to this point when discussing the properties of an ionization chamber.

The other dose specification now in use is the "absorbed dose" [3]), defined as "the amount of energy imparted to matter by ionizing particles, per unit mass of irradiated material, at the place of interest". It is expressed in "rads". One rad is defined as 100 erg/g, or 10^{-2} joule/kg. The total energy absorbed by a patient during exposure to radiation is called the "integral absorbed dose", and is usually expressed in kilogram-rads (not to be confused with kilorads); one kg rad is 10^5 erg or 10^{-2} joule.

The usual practice in X-ray therapy has been to measure the exposure dose, in roentgens. The absorbed dose in the skin and in deeper areas of the body can then be found with sufficient accuracy from tables and charts. Unfortunately this is scarcely practicable in the diagnostic use of X-rays. In the first place the tube voltage and amperage, filtration, and the size and location of the field are often varied several times in the course of each examination, making it virtually impossible to measure the total dose in roentgens. Another difficulty is the fact that the radiation used for diagnosis is not hard, as it generally is for X-ray therapy, but soft.

To explain this difficulty, and by way of introduction to the discussion of our dosemeter for

[3]) Report of the I.C.R.U. 1956, Handbook 62, Nat. Bur. Standards, Washington.

diagnostic use, we shall touch briefly on a few points concerning absorption. The absorption of X-rays is a function of their quantum energy. At a given quantum energy, however, a given substance always has the same absorption per gram/cm²; water in the liquid state, for example, absorbs just as much per gram/cm² as in the vapour state. (We are concerned with absorption in a thin layer whose thickness is expressed in mass per unit area.) The absorption can differ considerably from one substance to another, depending on the atomic number — the higher the atomic number the greater the absorption of radiation of given quantum energy — and on the relative quantities of the elements contained in the substance. The chemical binding of the elements plays no significant part. Air, water and wet tissue, for example, show roughly the same absorption per gram/cm². The absorption in bony tissue, which contains the heavier elements calcium ($Z = 20$) and phosphorus ($Z = 15$), is much greater. The absorption per gram/cm² is expressed by the *mass energy-absorption coefficient*, which is equal to the linear energy-absorption coefficient μ divided by the density ϱ. (Since there is no possibility of confuzion, we write simply μ in place of the approved symbol μ_{en}.)

The dependence of the mass absorption coefficient on the quantum energy of incident monochromatic X-radiation is shown in *fig. 1*. It can be seen that the curve is almost horizontal for hard radiation (high-energy radiation), but the variation of μ/ϱ with quantum energy is very marked for soft radiation. A similar curve is found for all substances.

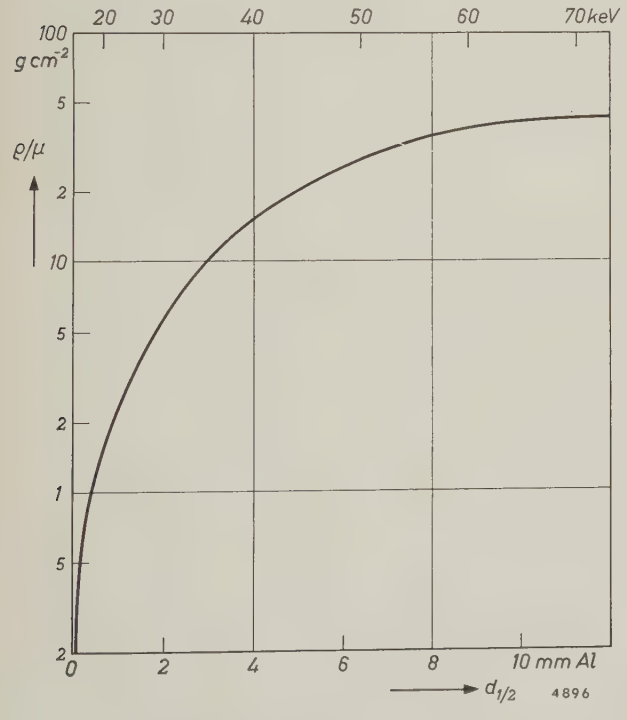

Fig. 1. The reciprocal of the mass-energy absorption coefficient μ/ϱ of air for monochromatic X-rays as a function of radiation quality. The latter is expressed as the half-value layer $d_{\frac{1}{2}}$ and also as the quantum energy (in keV). For hard radiation (as used in therapy) μ/ϱ is practically constant; for soft radiation (diagnostic) it varies considerably.

As the radiation from an X-ray tube is not monochromatic, it cannot be characterized by a single quantum energy. In practice the spectral intensity distribution — called the *quality* of the radiation — is specified by the thickness which a filter of aluminium or copper must have in order to reduce the dose rate (roentgens per unit time) to one half, one quarter, one eighth, etc., of the initial value. These thicknesses are termed the first, second, third, etc., *half-value layers* (HVL). In medical practice it is usual to determine only the first half-value layer (HVL_1).

The intensity of monochromatic (monoenergetic) radiation decreases exponentially with the mean free path in the absorber, and the quality of the radiation is therefore satisfactorily defined by HVL_1. The filter that reduces the intensity from $\frac{1}{2}$ to $\frac{1}{4}$ is then just as thick as the first, and so on. Where non-monochromatic radiation is concerned, the layers are successively thicker, the soft rays being most strongly absorbed and the remainder becoming progressively harder. The difference in thickness is greater the broader the radiation spectrum. The quotient HVL_1/HVL_2 is termed the homogeneity factor, and is thus unity for monochromatic radiation.

In fig. 1 the quality of the radiation is given along the abscissa in terms of both quantum energy and half-value layer. Although strictly applicable only to monochromatic radiation, each point of the curve is roughly valid for non-monochromatic radiation of the same HVL.

To indicate the specific difficulties encountered when integral doses of soft radiation are to be measured, we shall now consider the way in which the energy flux density, i.e. the energy per unit time passing through unit area of surface normal to the X-ray beam, is related to the ionization produced in air per unit time in that area. We note that the ionization is proportional to the *absorbed* energy: the above-mentioned ionizing energy of 34 eV per ion pair holds for all radiation qualities concerned. Since the energy absorbed per unit time in a small volume is equal to the product of the energy flux density and the absorption coefficient μ, we may infer that the relation between the dose rate in roentgens per unit time and the energy flux density contains the factor μ. This factor will of course vary with the quality of the radiation in the same way as μ/ϱ. We have seen from fig. 1 that μ/ϱ is practically independent of the radiation quality where the rays are hard (for therapy) but by no means so where the

rays are soft (for diagnostics). It is therefore understandable that the absorbed energy in an X-ray examination cannot easily be derived from the dose expressed in roentgens. For that to be possible the spectral intensity distribution of the X-rays would have to be known exactly.

With the diagnostic dosemeter to be described in this article the total energy incident on the patient can be accurately measured without its being necessary to know precisely the quality of the radiation used. Since the precision required in a measurement of the integral absorbed dose in diagnostics is not high — an uncertainty of 25% is permissible [1]) — this dose can be determined near enough by assuming that 20 or 30% of the incident energy is transmitted or scattered and the remainder absorbed [4]).

Although the gonad dose is obviously not determined in this way, it can be estimated if we know the total energy absorbed by the body, and the part of the body exposed to the rays (chest, stomach, etc.). Measurement of the integral absorbed dose is therefore a useful means of arriving at the gonad dose, which is itself very difficult to measure [5]).

The method by which the new dosemeter for diagnostics is made independent of the radiation quality will be discussed at the end of this article. First we shall consider a number of instruments for measuring therapeutic doses [6]).

Dosemeters for X-ray therapy

Ionization chambers

An ionization chamber for X-ray dosimetry is sketched in *fig. 2*. The cylinder wall *1* and the central pin *2*, both of which are conductive, form the electrodes mentioned in the introduction. Between them, fitted in an insulating bush *3*, is a third electrode *4*, in the form of a ring. This is given roughly the same potential as the central electrode and ensures that any leakage current across the insulation is not included in the measurement. In a calibration procedure, the chamber is given a carefully defined volume such that its sensitivity (in coulombs/roentgen) is conveniently adapted to that of the measuring equipment. In other words, full deflection of the meter is arranged to correspond with a round number of roentgens, say 3 or 10.

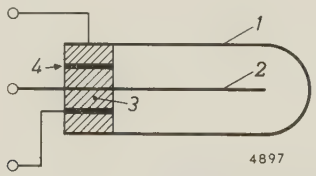

Fig. 2. Ionization chamber for dosimetry in therapeutic radiology (schematic). *1* wall. *2* central electrode. *3* insulation. *4* guard ring.

The current I that flows in an ionization chamber upon exposure to X-rays and the charge Q of the ions produced per unit time are proportional to one another below a certain critical value of Q. Above that value, I increases less than one would expect. The smaller the potential difference V between the electrodes *1* and *2*, the lower are the Q values at which this effect occurs (*fig. 3*). The reason for the effect is that the ions have a certain chance of recombining, thereby losing their charge. *Fig. 4* will help to make this clear.

This figure shows the relation between I and V for three different values of Q. At small values of V the current is seen to rise fairly steeply with the voltage (region A), after which it flattens out to an almost constant level (region B), and finally curves upwards again (region C). The explanation is that the ions travel relatively slowly at lower voltages (region A), so that many of them are able to recombine before reaching one of the electrodes. When the voltage is raised, the ions travel faster and thus have less opportunity to recombine; the current then rises until it becomes virtually independent of the applied voltage (region B). However, if V is raised to a value where the electrons in the electrical field inside the chamber absorb sufficient energy to produce ionization themselves, the newly formed ions add to the current, which thereupon rises again with V (region C). (This is the gas-amplification effect which underlies the operation of the proportional counter.)

As can be seen, the boundary between region B and region C lies at the same value of V at all three dose rates. This is not so as regards the boundary between A and B. With increasing V, the recombination effect persists at higher Q values, i.e. higher dose rates; there is then a greater concentration of ions and electrons and thus the ions individually have a greater chance of recombining.

It is now clear why the I-Q curves in fig. 3 begin to flatten out at high Q values. If Q is increased whilst V is kept constant, at a certain moment the boundary between the regions B and A (fig. 4) will

[4]) Cf. E. Zieler, Fortschr. Röntgenstr. **92**, 211, 1960. The fraction absorbed in various methods of chest examination is already known. See E. Zieler, *ibid.* **94**, 248, 1961.

[5]) See chapter IV (by J. Feddema and W. J. Oosterkamp) of the book "Modern trends in diagnostic radiology". (2nd series), Butterworth, London 1953, and also A. Neboschew and O. Schaft, Zur Überwachung der Patientenbelastung während der Röntgendurchleuchtung, Röntgen-Bl. **12**, 244, 1959.

[6]) For a thorough treatment of dosimetric methods in X-ray therapy and their physical background, see G. J. Hine and G. L. Brownell, Radiation dosimetry, Acad. Press, New York 1956.

be passed. This will happen less quickly the higher V is chosen (as long as V remains within region B, of course).

Besides the potential applied between the electrodes, another factor of importance in an ionization chamber of the type sketched in fig. 2 is the wall.

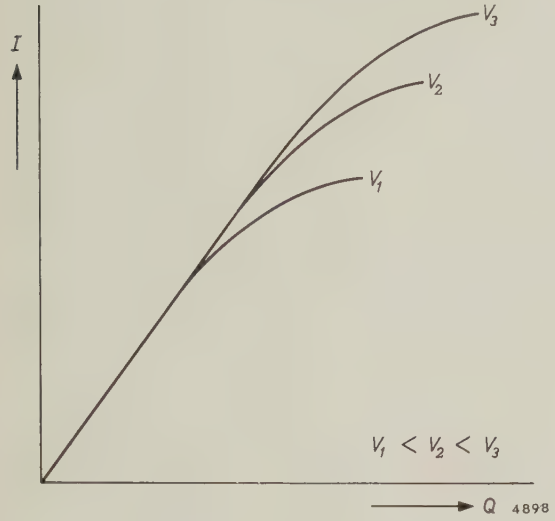

Fig. 3. Relation between the current I flowing in an irradiated ionization chamber and the charge Q produced by ionization per unit time, for various values of the applied voltage V.

It is for this reason that we have compared the current I with the charge Q produced per unit time in the chamber and not with the dose rate q. To explain this we recall the remark we made on the fact that the definition of the roentgen is based on the ionization caused by the secondary electrons generated in 0.001293 gram of air. Since these electrons have high kinetic energies — as we have already mentioned, the fastest acquire almost the total energy of the X-ray quantum — some of the secondary electrons liberated in the wall also enter the ion-collecting volume of the chamber and there contribute to the ionization of the air. On the other hand, some of the electrons formed in the air travel to the wall and contribute less to the ionization than would otherwise be the case. On the whole, these two effects are not entirely compensatory. In itself this would present no difficulties — the chamber must in any case be calibrated — if it were not for the fact that the resultant effect depends on the quality of the radiation. At constant V and constant true dose rate the current I of an ionization chamber is therefore dependent as a general rule on the quality of the radiation.

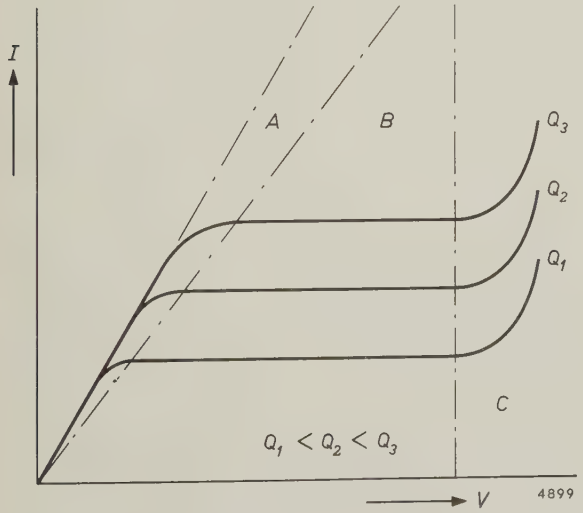

Fig. 4. Relation between the current I and the applied voltage V for various values of the charge Q formed per unit time in the chamber. The operating point should be in region B.

The wall also has another influence on the ion current: it absorbs part of the radiation, so that the intensity of the radiation inside the chamber is lower than the intensity at that spot in the absence of the chamber. This effect is again dependent on the quality of the radiation. By suitable choice of the wall material, the two wall effects can be made to compensate one another substantially in a particular range of radiation qualities [7]). In this way it is possible to build a chamber which has a reasonably constant sensitivity in a limited range of radiation qualities. This is sufficient for practical purposes, although of course more than one ionization chamber is needed to cover the whole range of therapeutically employed radiations. *Fig. 5* shows three of the ionization chambers of the Philips Universal Dosemeter, each of which is suitable for a specific range of radiation qualities. Particulars of their construction are given in *fig. 6*. Finally, *fig. 7* shows an ionization chamber fitted to the end of a 70-cm-long rubber tube for introduction into a body cavity, e.g. the oesophagus.

The increased ionization due to the secondary electrons liberated in the wall, and the decreased ionization due to secondary electrons penetrating the wall, compensate one another if the wall material and the gas filling have the same chemical composition. The difference in density is immaterial. If the wall and gas are not identical in chemical composition, then they must have the same mass absorption coefficient for X-radiation and the same atomic stopping power for electrons. In that case the wall is said to be equivalent to the gas filling. A wall that is equivalent to air for all qualities of radiation does not exist. As we have seen, the wall of the ionization chambers used in the Philips Universal Dosemeter is not meant to be entirely air-equivalent, the object being to compensate as far as possible for the absorption of X-rays in the wall.

[7]) See e.g. W. J. Oosterkamp and J. Proper, Acta Radiol. **37**, 33, 1952.

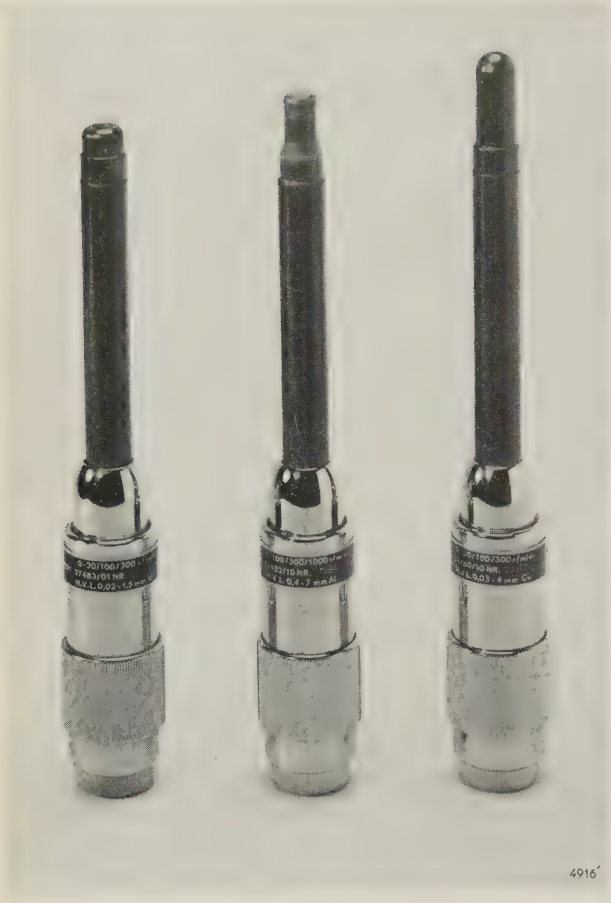

Fig. 5. Three of the ionization chambers of the Philips Universal Dosemeter. The one on the left is for dose rates up to 300 roentgens/second of radiation having a half-value layer (HVL) of 0.02 to 1.5 mm Al. The corresponding figures for the middle one are 1000 roentgen/min and 0.4 to 7 mm Al, and for the right-hand one 300 roentgen/min and 0.03 to 4 mm Cu. The ion-collecting space is at the top (cf. fig. 6).

The curve in *fig. 8* gives an idea of the extent to which the ionization current, at a given dose rate, is independent of the radiation quality. This is the correction curve applied to the reading given by the Philips Universal Dosemeter when fitted with the ionization chamber shown on the right in fig. 5 — a chamber used in deep therapy. The response for qualities between 0.2 and 1.5 mm Cu (i.e. roughly 5 and 20 mm Al, respectively; cf. fig. 1) is seen to vary by less than 1%. Even at 0.1 and 2.5 mm Cu, the variation is only 3%.

The ionization chambers which form a part of the Philips Universal Dosemeter are all calibrated before they leave the factory. This is done with an extremely stable (substandard) ionization chamber, the calibration curve of which is obtained by comparison with the standard ionization chambers [8]) at the National Physical Laboratory, Teddington (England), the Physikalisch-technische Bundesanstalt, Brunswick (Germany) and the Rotterdams Radiotherapeutisch Instituut (the Netherlands) [9]).

The calibration curve is constructed so as to ensure that the sensitivity of the Philips standard is equal to the average of the sensitivities of the three standard chambers mentioned and that of the National Bureau of Standards at Washington (U.S.A.). (The sensitivity of the latter standard chamber as compared with that of the National Physical Laboratory is given in the literature.) The maximum differences in sensitivity between the Philips substandard and these chambers (which occur at different radiation qualities in each case) are:

Nat. Phys. Lab.	0.9% higher
Nat. Bur. Stand.	0.5% higher
Rott. Radiother. Inst.	0.3% higher
Phys.-Techn. Bundesanst.	1.4% lower.

Only those ionization chambers are passed after calibration whose sensitivity for any given radiation quality differs by no more than 3% from the value found from the curve provided with the instrument (cf. fig. 8).

Condenser chambers

As we have seen, a condenser chamber is essentially a charged capacitor with a gaseous dielectric, which is gradually discharged upon exposure to

[8]) In a standard ionization chamber the wall plays no part whatsoever. The principle is described e.g. in the book by Hine and Brownell, quoted in note [6]).

[9]) Carried out in 1957 by W. J. Oosterkamp and J. Proper of Philips research laboratories at Eindhoven.

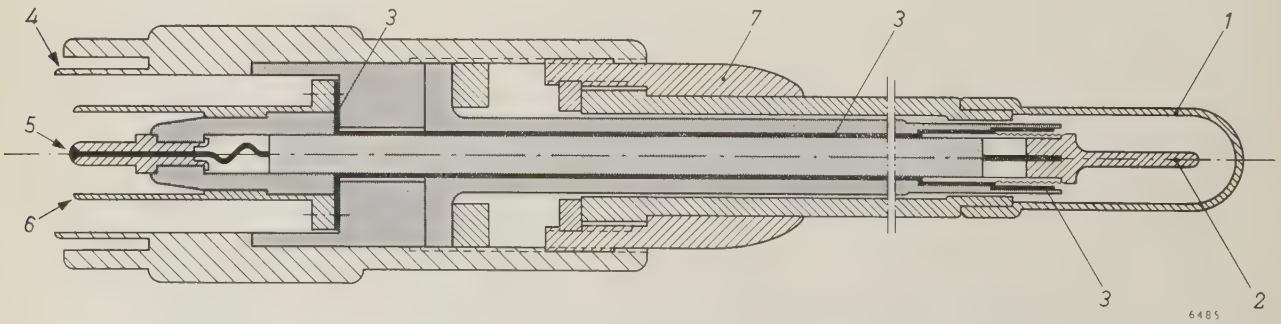

Fig. 6. Cross-section of one of the ionization chambers in fig. 5 (schematic). *1* chamber wall. *2* central electrode mounted on an insulating bushing with a ribbed surface to lengthen the creep path. *3* (thick black line) guard ring. *4*, *5* and *6* cable terminals, connected to electrodes *1*, *2* and *3* respectively. Except for the above-mentioned bushing, all insulating parts are shaded. The volume of the chamber can be adjusted to give the desired sensitivity by screwing the part *7*, fixed to the chamber wall *1*, in or out.

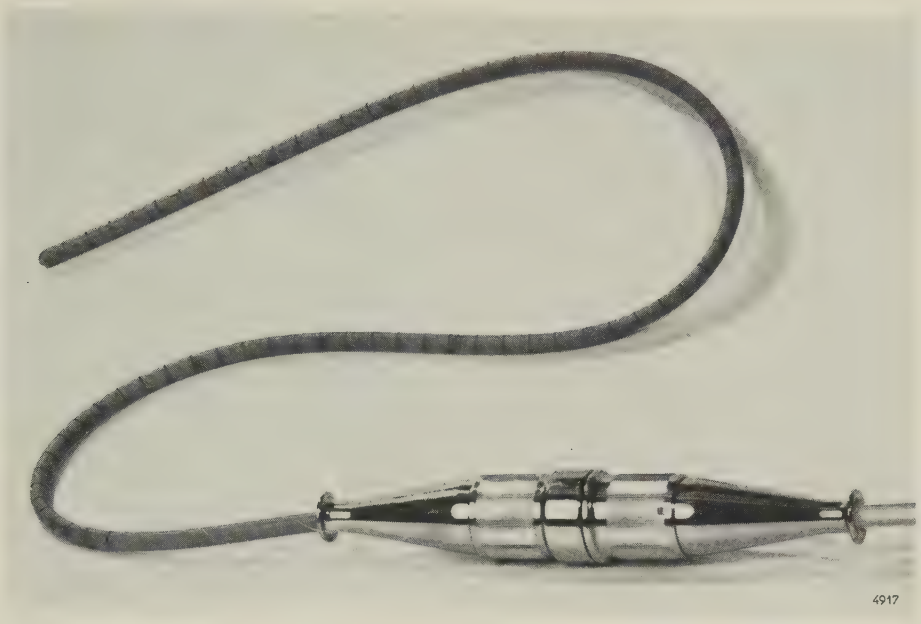

Fig. 7. For dose measurements in a body cavity, e.g. the oesophagus, a small ionization chamber is fitted to the end of a rubber tube 70 cm long.

radiation. Since a condenser chamber is not connected to the measuring circuit during exposure, it possesses no guard ring, and therefore special care must be paid to the insulation. It is necessary, for example, to ensure that the surface of the insulator is always kept dry.

From what has been said above about the effect of ion recombination on the measurement, it may be inferred that all values which the potential difference V of the electrodes acquires during a measurement must fall in the region within which the effect of recombination is not troublesome — region *B* in fig. 4. A condenser chamber must therefore not be discharged too far.

Like the chamber shown in fig. 7, condenser chambers can be used during therapeutic irradiations for dose measurements in body cavities. Very small ones are used for this purpose. Furthermore, as mentioned, they make it possible to measure doses at numerous places at the same time without having to use an equal number of measuring circuits.

Condenser chambers are also used as radiation monitors for personnel protection. They may then be carried around in the pocket, and serve as a means of ascertaining whether the measures of radiation protection adopted are in fact effective. Such chambers are usually given the convenient form of a fountain pen. Large condenser chambers, which are of course much more sensitive, are used for spot checks of the radiation level in places of work and also for detecting and measuring leakage radiation. Three types of condenser chamber are shown in

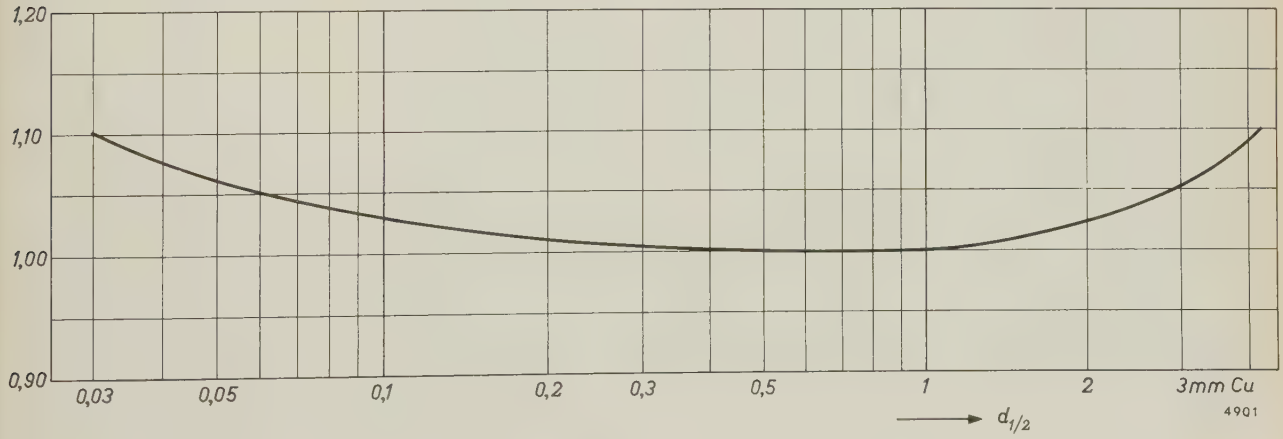

Fig. 8. The correction factor to be applied to the reading on the Philips Universal Dosemeter to find the actual exposure dose differs only very little from 1 in a fairly wide range of radiation qualities. The curve drawn here applies to the ionization chamber on the right in fig. 5.

fig. 9. The one on the right (see also *fig. 10*) has a very thin window (1 mg/cm^2) which makes it suitable for the measurement of very soft X-rays and β-rays.

Measuring circuit of the Philips Universal Dosemeter

The function of the measuring circuit associated with an ionization chamber is to give the electrodes — including the guard ring — the correct potential, and to give a direct reading of the ion current or of the charge. As an example, we shall discuss the circuit used in the Philips Universal Dosemeter. A diagram of the circuit, partly in block form, is shown in *fig. 11*. To measure a dose *rate*, switch S is turned to position *1*. The ion current then flows through resistance R, and the potential difference produced between the ends p and q of this resistance is measured with the circuit shown to the right of the broken line. Block *I* represents an electronic voltmeter. Since the current which this draws from the input circuit must be small compared with the ion current (which is itself of the order of 10^{-10} A) *I* must have a very high input resistance. This is achieved by making use of a vibrating-reed type of electrometer [10]).

[10]) See J. van Hengel and W. J. Oosterkamp, A direct-reading dynamic electrometer, Philips tech. Rev. **10**, 338-346, 1948/49. The circuit of the Philips Universal Dosemeter, largely developed by J. Fransen, differs in some points from the circuit described there, but is the same in principle.

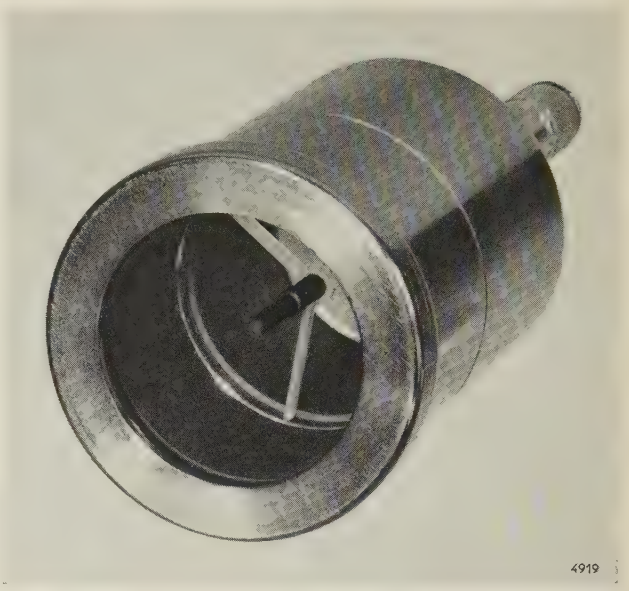

Fig. 10. Condenser chamber for very soft radiation with protective cap removed, showing the central electrode.

The output signal from *I* — an alternating voltage whose amplitude is proportional to the input voltage and whose frequency is equal to that of the vibrating-reed capacitor — is amplified in *II*, rectified in *III*, and applied to the moving-coil instrument *M*.

The sensitivity of the entire apparatus is stabilized by means of negative feedback, a variable portion of the output signal from *III* being fed back to *I* in antiphase by circuit *IV*. The sensitivity can also be varied in this way, which is desirable for two reasons. In the first place, it is then easy to switch over to another measuring range, and secondly there is no need to correct the reading of the meter if the temperature and pressure of the air differ from the values for which the chamber is calibrated. The correction required is made in advance by correspondingly altering the sensitivity of the measuring circuit.

The rectifying circuit *III* is both phase-sensitive and selective: it does not pass signals whose frequency differs from that of the vibrating capacitor, except for the

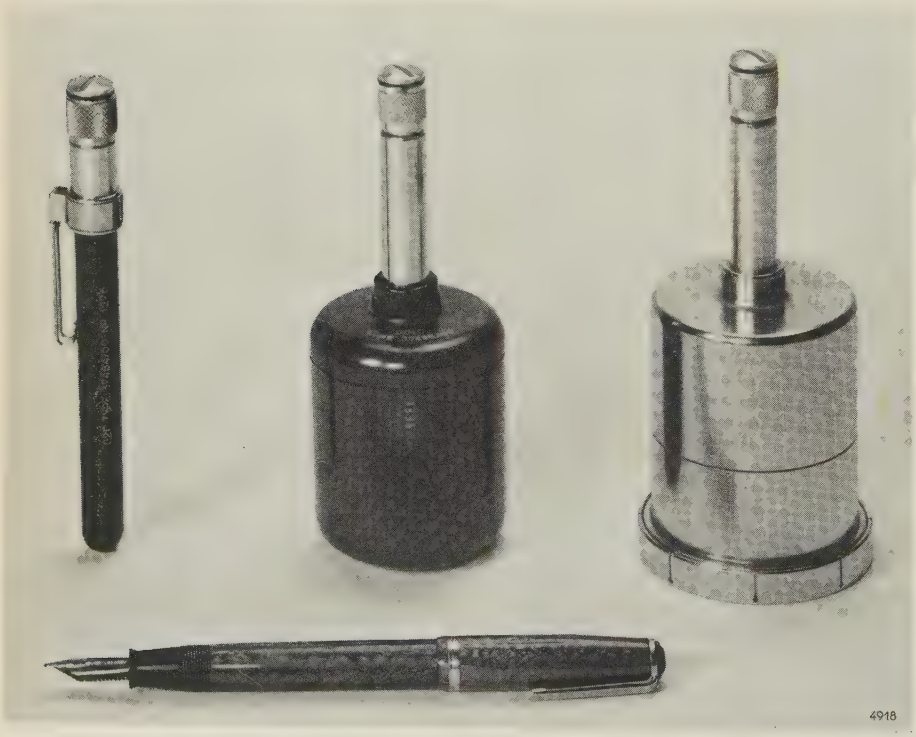

Fig. 9. Three condenser chambers used to monitor radiation for personnel protection. The smallest can be carried in the pocket like a fountain pen; the larger one in the middle, which is highly sensitive, can serve for measuring the radiation level in work places. The one on the right is for the detection of very soft X-rays and β-rays (cf. fig. 10).

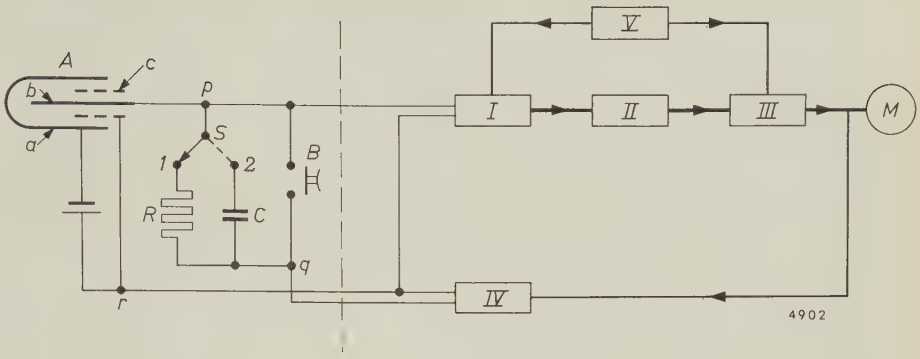

Fig. 11. Measuring circuit, partly in block form, of the Philips Universal Dosemeter. When the ionization chamber A (a is the wall, b is the central electrode and c the guard ring) is exposed to radiation, the ion current flows through the resistance R if switch S is turned to position *1*. The potential difference then appearing between points p and q is proportional to the ion current, and a measure of the dose rate. The potential is measured by a vibrating-reed electrometer I, amplified in II and rectified in III. The latter is a phase-sensitive rectifier which only passes signals having the frequency of the vibrating capacitor (and its odd harmonics). M meter. IV feeds a variable proportion of the output signal back to I in antiphase. This negative feedback stabilizes the amplification against mains fluctuations and makes it a simple matter to vary the sensitivity. V oscillator which drives the vibrating capacitor in I and supplies an auxiliary signal of the same frequency to III. When switch S is in position *2*, the ionization current is integrated and the dose in roentgens is measured. Push-button B serves to discharge the capacitor C after each measurement.

If it is desired to connect a condenser chamber between p and r, switch S must be set in a third position similar to position *2* but in which C has a much lower value.

odd harmonics. To achieve this, the output signal from the oscillator V, which drives the vibrating capacitor in I, is also fed to III. The object of making the circuit phase-sensitive is to prevent the negative feedback changing into positive feedback if the strength of the input signal should drop sharply, in which case the signal supplied by IV, which follows the change relatively slowly, may have a greater amplitude than the input signal itself. Owing to the fact that the circuit, for all practical purposes, only passes signals of the measuring frequency, interfering signals cannot affect the meter reading.

A detailed description of the operation and circuitry of blocks I, III and IV will be found in the article quoted under [10]).

If the *dose* and not the *dose rate* is to be measured, switch S is turned to position *2*. After the exposure, the voltage to which the ion current has charged the capacitor C is then measured and read off in roentgens.

For checking the operation of the circuit, a calibration device is incorporated in the Philips Universal Dosemeter. This is an ionization chamber, sealed off from the outside air and filled with nitrogen, which is connected to the electrometer circuit in the same way as the chamber used in the measurement. A small quantity of radium is applied to the central electrode; the radiation from this produces ionization in the nitrogen and causes a current of about 4×10^{-10} A to flow in the resistance R (fig. 11).

The sensitivity can be corrected for differences between the actual temperature and barometric pressure and those at which the chamber was calibrated by connecting to the circuit an ionization chamber which is in open communication with the atmosphere and in which the central electrode is fitted with a hollow glass bead containing radium (*fig. 12*). The α radiation emitted by the radium is absorbed in the bead wall; the β- and γ-radiation produce the ionization.

The correction can also be derived from a table if the pressure and temperature are accurately known.

A photograph of the Philips Universal Dosemeter is shown in *fig. 13*.

Fig. 12. Ionization chamber in open communication with the atmosphere and containing an internal radiation source for correcting the sensitivity of the measuring circuit (figs. 11 and 13) to allow for different values of temperature and air pressure.

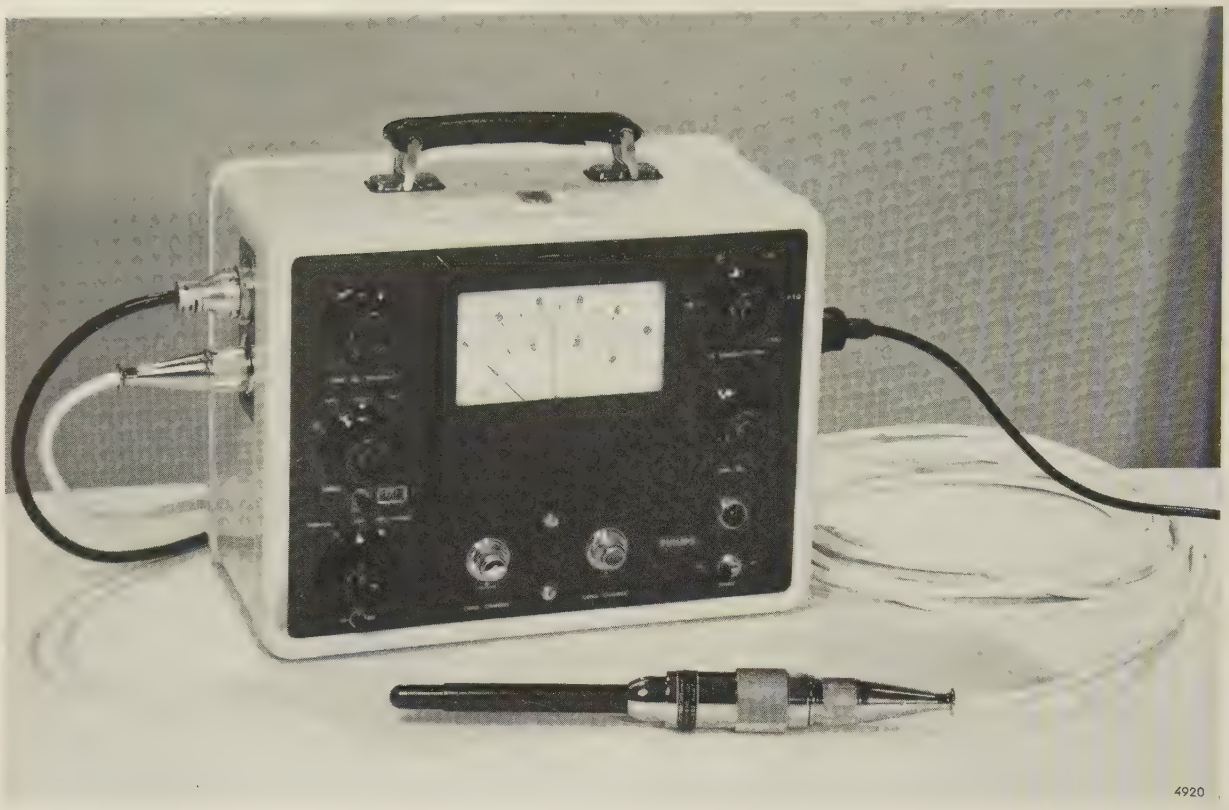

Fig. 13. The power supply and measuring unit of the Philips Universal Dosemeter, with one of the ionization chambers connected to it. On the right of the front panel can be seen, from the bottom upwards: mains switch, signal lamp, control for zero adjustment, control for sensitivity correction. On the left: push-button B and switch S (fig. 11), push-button for switching on the calibration device, range selector switch, and control for zero adjustment of any recording apparatus that may be connected. A condenser chamber can be connected to the terminals underneath the meter, after removing the protective cap. The terminal on the right is for charging the chamber, the one on the left for measuring the residual charge. The black cable on the right is the mains lead. The plug top-left carries the lead to a recording instrument.

A dosemeter for diagnostic use

We now come to the dosemeter for diagnostic use. As mentioned, this instrument measures the total radiant energy incident on the patient. For this purpose the detector is given the form of a large flat box, which is placed in front of the patient. The box is large enough to transmit the entire X-ray beam. The instrument is made independent of the quality of the radiation by using two ionization chambers separated by a filter. Provided certain conditions are fulfilled, the difference between the ion currents of the two chambers is proportional, over a fairly wide range of radiation qualities, to the energy flux incident on the patient [11]). The conditions to be fulfilled will be examined with reference to *fig. 14*.

In this figure, electrodes *1* and *2* together form the first ionization chamber (P), and the second (S) is formed by electrodes *3* and *4*. Both chambers are fitted with the usual guard ring (*5* and *6*). The respective distances between the electrodes are d_P and d_S. The X-ray beam (shaded) passes from the focus A successively through chamber P, filter B and chamber S. Electrodes *2* and *3* in the two chambers are interconnected, and the voltages are applied with opposite polarities. The output terminals p and r are connected to a measuring circuit using negative feedback, in the same way as the single ionization chamber in fig. 11 is connected to the circuit in the Philips Universal Dosemeter. (The corresponding points in this figure are also denoted by p and r.)

When a suitable voltage is applied between electrodes *1* and *2* (fig. 4), the charge produced per unit time in chamber P is equal to the current I_P and depends on the energy flux E_P at the place of interest according to the equation:

$$I_P = e \times \mu \times d_P \times \dot{E}_P / W = C\, \mu\, d_P\, \dot{E}_P \,. \quad . \quad (1)$$

[11]) This idea was the fruit of a discussion between one of the authors and K. Bronsema, X-ray and Medical Apparatus Division, Eindhoven.

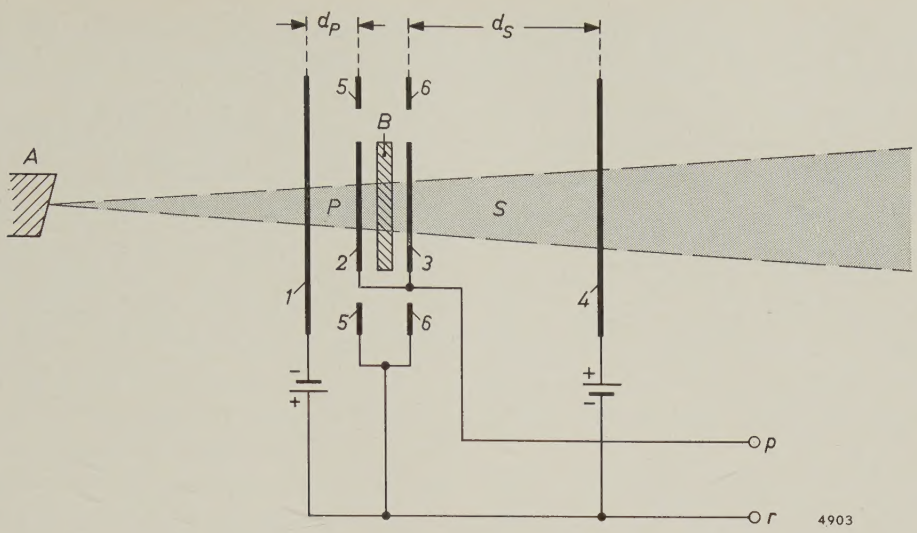

Fig. 14. Twin ionization chamber for measuring integral doses in X-ray examinations. The X-ray beam (shaded) passes from the anode A through the ionization chamber P (electrodes *1* and *2*), the filter B and the ionization chamber S (electrodes *3* and *4*). The chambers have the form of a flat box and are large enough to transmit the whole of the X-ray beam incident on the patient. Electrodes *5* and *6* are the guard rings.

Here e is the elementary charge, W the energy required to produce one ion pair — 34 eV in air — and C is the ratio e/W. Similarly, for chamber S we have:

$$I_S = C\,\mu\,d_S\,\dot{E}_S. \qquad \ldots\ldots \quad (2)$$

The difference between the two currents is:

$$I = I_S - I_P = C\,\mu\,(\dot{E}_S\,d_S - \dot{E}_P\,d_P)\,. \qquad . \quad (3)$$

Disregarding the absorption in the walls, $\dot{E}_S/\dot{E}_P$ is equal to the transmission factor α of filter B. Equation (3) may therefore be written

$$I = C\,\mu d_S \dot{E}_S \left(1 - \frac{1}{\alpha\beta}\right), \qquad \ldots\ldots \quad (4)$$

where $d_S/d_P = \beta$. In these equations, μ and α both depend on the quality of the radiation; α is greater and μ smaller the harder are the rays.

If the factor $\mu(1 - 1/\alpha\beta)$ is independent of the radiation quality, so too is the relation between I and $\dot{E}_S$. Since we are perfectly free to choose the value of β, and can also control the form of the variation of α within certain limits by a suitable choice of the thickness and material of the filter, this requirement can be exactly fulfilled for two qualities of radiation, and met to a fair approximation for the radiation in the neighbouring range.

Fig. 15 illustrates the extent to which the response of the apparatus so designed is independent of the radiation quality. The ratio between the response and the energy flux leaving the chamber is plotted as a function of the anode voltage of the X-ray tube [12]). At voltages of 55 and 130 kV (HVL respectively 2.3 and 6.3 mm Al) the reading is seen to be exact, and between these values it deviates by no more than about 15%. The values of certain quantities governing the performance are given in the caption to fig. 15.

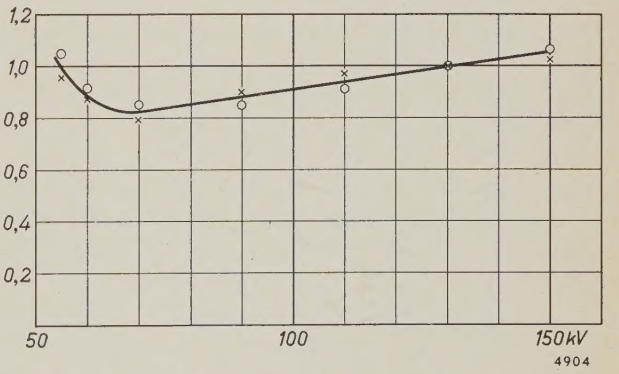

Fig. 15. Correction factor to be applied to the reading of a diagnostic dosemeter using a twin chamber. In a wide range of radiation qualities this factor differs only slightly from unity. (The half-value layers corresponding to anode voltages 50, 130 and 150 kV are 2.3, 5.6 and 6.3 mm Al, respectively.) The points × were obtained with a scintillation detector, the points ○ were calculated from the dose in roentgens measured with an ionization chamber and from the relevant value of μ. (The experimental instrument was fitted with an aluminium filter $1\frac{1}{2}$ mm thick. At 50 kV its transmission factor α is 0.50, at 130 kV it is 0.74. Distances between electrodes: d_P = 2.0 mm and d_S = 4.5 mm).

---

[12]) See K. Reinsma, Dosismeters voor de röntgendiagnostiek, Centrex Publishing Co. Eindhoven 1960, where further particulars will be found. (To be published shortly in English.)

The experimental points in fig. 15 were obtained by two entirely different methods. The first method [13]) used a scintillation counter and count-rate meter. Before the actual measurements were made, the response of the measuring equipment was determined by exposing the detector to monochromatic X-radiation — obtained by diffraction in a crystal platelet — and counting the individual quanta. The energy flux corresponding to a given reading on the meter could then be directly computed from the number of quanta counted and the known quantum energy. This was done with tungsten and molybdenum $K\alpha_1$ radiation.

The sensitivity of the twin chamber to monochromatic tungsten and molybdenum radiation was also determined. By then repeating the measurement with non-monochromatic radiation it was found that it made no difference to the response of the twin chamber whether it was exposed to monochromatic or non-monochromatic radiation, provided the half-value layers of both were identical and provided, of course, that the energy fluxes determined with the aid of the scintillation instrument were also identical. It was accordingly assumed that the same would apply to all quantum energies involved, and the measurements from which the curve in fig. 15 was plotted were therefore done with non-monochromatic radiation.

The measurements were also carried out with an ionization chamber instead of a scintillation counter. The energy flux (see equation (1)) was then determined from the measured dose rate and the value of μ found for the radiation used. This value was found by again considering the radiation as monochromatic radiation of the same half value layer [14]). As appears from fig. 15, the results obtained by both measurements are quite close.

Although the negative-feedback electrometer circuit for the twin chamber broadly resembles that in the Philips Universal Dosemeter, there are several important differences. Firstly, an electrometer pentode, type 4068, is used instead of a vibrating-reed capacitor. This tube is biased to give a grid current of about 3×10^{-15} A, corresponding to only 0.1% of the smallest difference current measured in practice. Secondly, the current is always integrated. The instrument thus indicates the total energy incident on the patient since the beginning of the examination, and not the energy flux. Further particulars will be found in the publication quoted under [12]).

Several experimental dosemeters for diagnostic use have been built at Eindhoven on the principle described, and have already been used in various hospitals. An instrument of this kind will be marketed in the not too distant future.

[13]) Developed in cooperation with C. Albrecht of Philips Research Laboratories and A. F. J. van Himbergen of the X-ray and Medical Apparatus Division, Eindhoven.

[14]) Use was made of the data presented in the I.C.R.U. report mentioned in note [3]).

Summary. In recent years it has proved desirable to measure the X-ray dose administrated to a patient not only in therapeutic irradiations but also in diagnostic examinations. In therapeutic practice the dose received by a given part of the body is found from the exposure dose measured in roentgens, which is directly related to the ionization produced by the rays in air. A description is given of the ionization chambers and electrometer circuit of the Philips Universal Dosemeter, which can be used for this purpose. In X-ray examinations, it is impracticable to measure the dose in this way. A dosemeter for diagnostic use is described which measures the total radiant energy incident on the patient during an examination. From this it is possible to determine with sufficient accuracy the integral absorbed dose, i.e. the energy absorbed by the patient (unit: kg rad = 10^{-2} joule).

ABSTRACTS OF RECENT SCIENTIFIC PUBLICATIONS BY THE STAFF OF N.V. PHILIPS' GLOEILAMPENFABRIEKEN

Reprints of these papers not marked with an asterisk * can be obtained free of charge upon application to Philips' Electrical Ltd., Century House, Shaftesbury Avenue, London W.C. 2, where a limited number of reprints are available for distribution.

2835: J. G. van Wijngaarden: A travelling-wave tube for the frequency band of 3800 to 5000 Mc/s (Le Vide **15**, 36-40, 1960, No. 85; in French and in English).

Details are given of the construction of a travelling-wave tube for the frequency band mentioned. The theory is assumed to be known. Particular mention is made of glass-to-metal seals, alignment and degassing, and the design of the permanent magnet. The object of the design, which is to produce a tube that can be replaced without requiring adjustment, whose life should exceed ten thousand hours, which should possess constant characteristics and have a well-screened magnetic field, is achieved through the use, among other things, of a dispenser cathode (L cathode).

2836: B. B. van Iperen: Reflex klystrons for millimeter waves (Proc. Symp. on millimeter waves, New York, March 31, April 1 and 2, 1959, pp. 249-259, Polytech. Inst. Brooklyn, 1960).

See Philips tech. Rev. **21**, 221-228, 1959/60.

2837: H. J. Prins: Transforms for finding probabilities and variate values of a distribution function in tables of a related distribution function (Statistica neerl. **14**, 1-17, 1960, No. 1).

In statistics, distribution functions are used which can often be transformed one into the other by means of suitable substitutions. This article gives the transforms for the most familiar distributions. With their aid, statisticians are enabled to add to existing tables. Knowledge of the relations between the distributions can also provide more insight into certain methods of statistical testing.

2838: J. S. C. Wessels and H. Baltscheffsky: Adenosine triphosphatase activity in chloroplasts (Acta chem. scand. **14**, 233-246, 1960, No. 2).

Adenosine triphosphate (ATP) was added to a suspension of spinach chloroplasts, and also $MgCl_2$ in some experiments. Inorganic phosphate was then split from the ATP at a temperature of 30 °C, and the amount of phosphate produced after a certain time was determined colorimetrically. The experiments were done with several chloroplast preparations, and the influence of pH was investigated in each case. The reaction is attributed to an enzyme present in the chloroplasts, here referred to as ATP-ase. At $p\mathrm{H} = 7.5$ the activity of the preparations tested was more or less identical. It was greatly stimulated by $MgCl_2$ and inhibited by chlorpromazine. The reaction in the presence of $MgCl_2$ was also investigated kinetically. Experiments in which ATP was replaced by Na pyrophosphate exclude the possibility that the ATP-ase activity at $p\mathrm{H} = 7.5$ involves a liberation and a subsequent hydrolysis of inorganic pyrophosphate. At $p\mathrm{H} = 5.5$ the activity differed considerably from one preparation to another, and was not sensitive to $MgCl_2$ and chlorpromazine.

The question is also considered whether a functional relation exists between the investigated reactions and the enzymatic mechanism by which phosphorylation of adenosine diphosphate (ADP) is coupled to electron transport during light-induced phosphorylation.

2839: J. Hornstra: Models of grain boundaries in the diamond lattice, II. Tilt about $<001>$ and theory (Physica **26**, 198-208, 1960, No. 3).

Models are presented for large-angle grain boundaries with a $<001>$ tilt axis. For all angles of tilt, dislocations without dangling bonds can be used in the construction of these models. One model may be considered either as an array of edge dislocations or as an array of 45° dislocations. In the last section the crystallography of regular grain boundaries is discussed, the grain-boundary index is introduced and the application of the transformation matrix to grain-boundary problems is illustrated.

2840: M. Koedam: Sputtering of single crystal metals bombarded with rare gas ions of low energy (50-350 eV) (Proc. 4th int. conf. on ionization phenomena in gases, Uppsala 17-21 August 1959, edited by N. Robert Nilsson, pages ID 252-ID 254, North-Holland Publ. Co., Amsterdam 1960).

Single crystals of Cu and Ni have been bombarded

with rare-gas ions of low energy. The directional distribution of the atoms sputtered from a (111) and a (110) surface bombarded with normally incident ions have been determined. Certain preferential sputtering directions are found. The sputtering yield in the preferential (110) direction has been determined as a function of the ion energy (50-350 eV) for Kr^+, Ar^+ and Ne^+ ions.

2841: G. J. M. Ahsmann and Z. van Gelder: The normal cathode fall on single crystal cathodes (as **2840**, pp. ID 266-ID 268).

A glow discharge has been applied to a number of single-crystal cathodes. For most crystals the burning voltage depends on the orientation of the crystal face. Some crystal faces, such as the (100) face of germanium, are not stable but become somewhat roughened by the discharge; it appears that there is a tendency for another crystal face to be exposed by sputtering, probably the (111) face.

It is shown that it is possible to obtain very reliable and stable values of the normal cathode fall by using single-crystal cathodes.

2842: M. Klerk: A contribution to the investigation of the striated positive column (as **2840**, pp. IIA 283-IIA 285).

An experimental investigation of the striated column of low-pressure DC discharges and HF discharges in the range 10-30 Mc/s has led to the conclusion that the origin of the striations is principally seated in the plasma of the column itself. In some cases, however, the boundary conditions at the ends of the column cause a disturbance of the plasma and so give rise to the occurrence of striations.

2843: G. J. M. Ahsmann: The impedance and recovery time of glow discharges in mixtures of rare gases (as **2840**, pp. IIA 309-IIA 313).

It is shown that the complex impedance of a glow discharge in a rare gas is considerably reduced by the addition of another rare gas with a lower ionization potential than the main gas. Both the real and the imaginary part decrease. It is shown that the self-inductance of the discharge decreases in inverse proportion to the mobility of the ions in the Crookes dark space.

The addition of a rare gas with a lower ionization potential than the main gas also has a large effect on the recovery time of the discharge.

2844: Th. P. J. Botden: A decade indicator glow-discharge tube operating on signals of low current and voltage (as **2840**, pp. IID 443-IID 447).

See Philips tech. Rev. **21**, 267-275, 1959/60.

2845: O. Reifenschweiler: Massenspektrometrische Untersuchungen der Ionenemission und Ionenverteilung von Gasentladungsplasmen (as **2840**, pp. IIE 541-IIE 548). (Research on ion emission and ion distribution of gas-discharge plasmas by means of mass spectrometry; in German.)

A method is discussed for investigating the ion emission from gas-discharge plasmas, enabling conclusions to be drawn on the ion-density distribution inside the plasma. Both radio-frequency and arc discharges in hydrogen are used. An ion-extraction system and an electrostatic-lens system produce an image of the plasma boundary, and the current-density distribution of the various types of ions is measured along the diameter of this image. The relative contributions of different ions are found to differ strongly. A relatively weak magnetic field perpendicular to the discharge axis causes the emission maxima of the plasma boundary to shift, the extent of the shift varying with the type of ion. Finally a movable extraction probe is described, suitable for the determination of ion densities at arbitrary points inside the plasma.

2846: C. Z. van Doorn: Thermal equilibrium between F and M centers in potassium chloride (Phys. Rev. Letters **4**, 236-237, 1960, No. 5).

Single crystals of KCl (measuring $4 \times 5 \times 1.3$ mm) were heated to 697 °C in potassium vapour at various pressures. A heating time of ten minutes was sufficient to obtain equilibrium, after which the high-temperature equilibrium was frozen in by rapid quenching in CCl_4. The absorption of the F and M bands was measured at 77 °K. The M concentration was found to vary quadratically with the F concentration, which is in agreement with the $2F \rightleftarrows M$ equilibrium (Van Doorn and Haven) and inconsistent with the assumed equilibrium F + vacancy pair $\rightleftarrows M$ (Seitz-Knox model). A rough determination of the equilibrium constant $K' = [M]/[F]^2$ at different temperatures showed the temperature dependence to be small, corresponding to a heat of formation of the M centres of about 0.01 eV.